



Department of Mechanical and Aerospace Engineering

Exploring the potential of small-scale District Heating schemes based on renewable sources: A modelling approach based on an existing scheme at Findhorn Ecovillage.

Author: Eleftheria Vavoura

Supervisor: Graeme Hamilton Flett

A thesis submitted in partial fulfilment for the requirement of the degree

Master of Science

Sustainable Engineering: Renewable Energy Systems and the Environment

2019

Copyright Declaration

This thesis is the result of the author's original research. It has been composed by the author and has not been previously submitted for examination which has led to the award of a degree.

The copyright of this thesis belongs to the author under the terms of the United Kingdom Copyright Acts as qualified by University of Strathclyde Regulation 3.50. Due acknowledgement must always be made of the use of any material contained in, or derived from, this thesis.

Signed

A handwritten signature in blue ink, appearing to read 'E. B. B. B. B.', enclosed in a rectangular box.

Date: 23/08/2019

“‘The best’ is the enemy of ‘good’.”

-Aristotle

“Always pursue the laborious efforts that lead to great and brilliant achievements for the society.”

-Democritus

New ideas, technologies, and discoveries, as well as environmental phenomena will always come forth and change our minds, our studies, and the way we react and adjust to the world around us.

This does not imply, however, that we should stop trying to provide solutions for our current and future problems, with the means and knowledge available to us today.

Abstract

Driven by the focus of the UK on large District Heating systems, which take long years to be developed and are still based mostly on gas as a fuel, an effort was made in this project to develop a modelling methodology that could be applied to small scale district and decentralised schemes, integrating efficient and renewable systems.

Based on an existing system at Findhorn Ecovillage in Scotland, a MATLAB model was developed for this purpose, modelling separately an air source heat pump, solar thermal flat plate collectors and a stratified water storage tank. The methodology was based on mostly steady state approaches found in literature and inspired by recent studies of decentralised and low temperature district heating systems.

The work done over just under three months resulted in a mostly functional model, especially in terms of the heat pump and storage, and a much better understanding of the complexities of such systems, that could fuel future work.

Acknowledgements

First of all I would like to sincerely thank my supervisor Mr Graeme Flett for his guidance, advice, and useful inputs he provided me with throughout our meetings for this project

Secondly, I would like to thank the rest of my instructors in this MSc degree at the University of Strathclyde, as well as my classmates, for making this past year in Scotland an unforgettable experience for me.

Finally, I am eternally grateful to my family and friends for always supporting me through the good and the bad, and for always being by my side.

List of Figures

| | |
|---|----|
| Figure 1. Heat generation in EU-28 by fuel (1990-2016). | 15 |
| Figure 2. Fuel mix of DH schemes in the UK. (Chauvaud De Rochefort, 2018)..... | 16 |
| Figure 3. Average daily DHW consumption for typical households of various sizes and compositions. (BRE Housing Centre, 2005) | 18 |
| Figure 4 Daily DHW consumption data for UK dwellings (). | 19 |
| Figure 5. Solar beam radiation on a horizontal surface ($\beta=0$) & on a tilted surface ($\beta>0$). (Duffie & Beckman, 2013)..... | 21 |
| Figure 6. A schematic of the heat transfer procedures between a flat plat collector & its environment. (Quaschnig, 2016) | 21 |
| Figure 7. Optical efficiencies and heat loss coefficients of typical solar collectors. (Quaschnig, 2016) | 23 |
| Figure 8. Series-parallel (left) and parallel (right) connection configurations for a field of FPCs (Zelzouli, et al., 2012)..... | 24 |
| Figure 9. A graphical representation of how a thermal energy system operates as part of a heating system . (Kalaiselvam, et al., 2014)..... | 25 |
| Figure 10. A water storage tank with an immersed solar coil. (Kalogirou, 2014) | 26 |
| Figure 11. A hypothetical stratified tank with N=5 nodes and an inlet flow. (Duffie & Beckman, 2013)..... | 27 |
| Figure 12. Layout of a nodal model for a stratified water tank. (Kleinbach, 1990) | 28 |
| Figure 13. The operation temperatures of a heat pump. (Reinholdt, et al., 2019)..... | 30 |
| Figure 14. Commonly used diversity factor curves for heat networks. () | 32 |
| Figure 15. A schematic of single (left) & twin (right) DH pipes.. (van der Heijde, et al., 2017) | 33 |
| Figure 16. The COP of the chosen heat pump for the baseline scenario as a function of the ambient air and output water temperatures..... | 40 |
| Figure 17. Charging schedule vs Grid carbon intensity for 2 weeks in January. | 43 |
| Figure 18. Classification of UK grid carbon intensity in several categories for the years 2017-2019. () | 44 |
| Figure 19. A panoramic view of Findhorn Ecovillage. (Ecovillage Findhorn, n.d.)..... | 45 |
| Figure 20. Baseline Scenrio total SH demand. | 50 |
| Figure 21. SH Demand of each flat (February week)..... | 51 |
| Figure 22. Baseline Scenario total DHW demand..... | 51 |
| Figure 23. Scenario 1 total SH demand. | 52 |
| Figure 24. Scenario 1 total DHW demand | 53 |
| Figure 25. . Scenario 2 total SH demand. | 53 |
| Figure 26..... | 54 |
| Figure 27. Baseline Scenario storage tank (February week). | 55 |
| Figure 28. Baseline Scenario storage tank (July week). | 56 |
| Figure 29. Performance comparison between the ASHPs of the individual DH schemes (Scenario 1). | 56 |
| Figure 30. Performance of the shared ASHP (22kW) (Scenario 2). | 57 |

List of Tables

| | |
|--|----|
| Table 1. Draw-off categories and their respective mean flow rates, standard deviation, and time durations(). | 34 |
| Table 2. Geometrical specifications of the existing buildings of the Case Study. | 46 |
| Table 3. U-values of the building envelopes. | 48 |

Abbreviations

| | |
|------|--------------------------------|
| CHP | Combined Heat & Power |
| DF | Diversity Factor |
| DH | District Heating |
| DHW | District Hot Water |
| EC | Energy Centre |
| FPC | Flat Plate Collector |
| RES | Renewable Energy Systems |
| SH | Space Heating |
| SS | Substation |
| STES | Sensible Thermal Energy System |
| WST | Water Storage Tank |

Contents

| | |
|--|----|
| Copyright Declaration | 2 |
| Acknowledgements | 6 |
| List of Figures | 7 |
| List of Tables..... | 8 |
| Abbreviations | 8 |
| 1. Introduction | 11 |
| 1.1. Project Aims | 11 |
| 1.2. Methodology Overview | 12 |
| 1.3. Thesis Structure | 14 |
| 2. Literature Review | 15 |
| 2.1. Low Carbon Heat scene in Europe | 15 |
| 2.1.1. Renewable Energy Systems integration | 15 |
| 2.1.2. The situation in the UK | 16 |
| 3. Technical Background..... | 17 |
| 3.1. Heat Consumption in domestic buildings..... | 17 |
| 3.1.1. Domestic Hot Water Consumption..... | 17 |
| 3.1.2. Energy Consumption for Space Heating | 19 |
| 3.2. Solar Thermal Systems..... | 20 |
| 3.2.1. Solar Flat Plate Collectors | 21 |
| 3.2.2. Sensible Thermal Energy Storage | 24 |
| 3.3. Air Source Heat Pumps | 30 |
| 3.4. Heat Distribution networks..... | 31 |
| 4. Method..... | 34 |
| 4.1. Assessing Heat Demand in Domestic Buildings | 34 |
| 4.1.1. Domestic Hot Water Demand Analysis..... | 34 |
| 4.1.2. Space Heating Demand Analysis | 35 |
| 4.2. Heating System Modelling Approach | 35 |
| 4.2.1. Solar Collector Model | 36 |
| 4.2.2. Thermal Energy Storage Model | 37 |
| 4.2.3. Heat Pump Model..... | 39 |
| 4.2.4. District Heating Network | 41 |
| 4.2.5. Supply – Demand Matching | 41 |
| 4.3. Assessing Costs & CO ₂ Emissions | 43 |
| 5. Case Study: Findhorn Ecovillage | 45 |
| 5.1. Examined Buildings | 45 |

| | |
|---|----|
| 5.2. Examined Heating Scheme..... | 46 |
| 5.3. Cost of electricity | 47 |
| 6. Simulated Scenarios | 48 |
| 6.1. Baseline Scenario | 50 |
| 6.2. Scenario 1: Individual systems for neighbouring clusters of buildings..... | 52 |
| 6.3. Scenario 2: Shared system for neighbouring clusters of buildings..... | 53 |
| 7. Results & Discussion..... | 55 |
| 8. Conclusions & Future Work..... | 58 |
| References..... | 60 |
| APPENDIX A | 64 |

1. Introduction

1.1. Project Aims

The first aim of this project was to create a middle ground between the “black box” approach followed by some commercial software used in modelling district energy systems and the complex, highly detailed approach of advanced software used for the same purpose in research fields.

This could be achieved by a model that is straightforward and easy to comprehend and adapt to different demand characteristics, system specifications, and operational conditions. Hopefully this would provide a basis for trying out how supply systems with different sizes and performance parameters could be combined, in order to cover the heat demand of a certain number of buildings.

Eventually, a model was developed, based on a specific configuration of an existing development in Scotland. The focus was not on creating an accurate simulation tool, but a tool that would allow some experimentation with different capacities and performance characteristics of individual systems. Which is why the control part was kept as simple as possible, yet based on relevant research literature, which deals with similar combinations of energy systems as the one investigated in this project.

1.2. Methodology Overview

The first step of this project was to review literature relevant to district heating and building systems supplied by renewable resources, and investigate existing projects. Then the research focussed on the developed methodologies for modelling district heating schemes and, specifically, their individual systems. A real-life project that could be used as a case study was provided by the Energy Systems Research Unit, along with annual demand data and some fundamental information about the characteristics of the buildings and the existing, small-scale DH system. Based on the energy sources and configurations used in that system, 1-D, mostly simplified methods were chosen and studied in depth, in order to model the performance of the individual systems and connect them with each other and with the buildings.

Later on, a model began to take form on the programming environment MATLAB 2016a. The choice was made in this study to model each system individually, in an effort to capture the essence of each system's operational principles. Separate functions were created for the heat pump, solar thermal panels, and storage tank employed. The performance of these energy systems was calculated according to a steady-state approach that is often followed in relevant literature. This modelling approach is based on the performance parameters determined by the manufacturers through testing each system with regard to EN/ISO standards, so that it would not go into too much complexity and would be easier to apply to different systems with known performance parameters.

The control strategy was kept the same control decisions made by research teams experimenting with the performance of similar schemes, including roughly the same individual systems and principles. Flow rates were included in the modelling, in order to interconnect the systems in a more realistic way, but were kept constant, so that the resulting model would not be unnecessarily complex.

For simplicity reasons, and due to lack of data of high time-resolution that could be used as inputs, an hourly time resolution was used.

Heat demand profiles based on generic space heating profiles for the UK, adjusted to the weather conditions of the year under study through the Degree Days Method, and

on the assumptions of the DHW Calc tool, developed by the University of Kassel. MS Excel was used for data analysis and for producing representative figures.

In retrospect, the methodology followed was proven to be rather too spread out and complicated for the timeframe of this individual project. However, some reasonable results were produced. Additionally, the resulting model on MATLAB is functional and quite flexible, so it could be easily improved with some further work.

1.3. Thesis Structure

In Chapter 2 of this thesis, a review is made of the current conditions regarding low carbon energy supply in Europe, while Chapter 3 includes a detailed review of the relevant technical literature, listing and briefly describing all the analysis methods and main equations that are later used by this study.

Chapter 4 goes one step further, building on Chapter 3 by explaining the specific approach this specific study followed, including all the necessary assumptions that were made in the progress.

The Case Study in which the methodology was applied -a District Heating scheme supplying a small number of flats and bungalows in Findhorn Ecovillage, Scotland- is presented in Chapter 5, along with some basic information about the buildings under study. The fundamental operational principles of the heating scheme are also explained, as well as the grid electricity costs considered.

In Chapter 6, the specific assumptions and arithmetic values of key parameters, which were applied for all investigated scenarios, are listed. Afterwards, the demand characteristics and profiles, as well as the topology and individual system specifications, are explained, in dedicated subsections for each scenario.

The results are presented and discussed in Chapter 7. The focus lies on the behaviour of the systems during characteristic weeks of the year, and on highlighting the average monthly COP values achieved by the heat pumps of the different scenarios during the simulation year.

In Chapter 8, the limitations of the model are recognised and some suggestions made for future study based on a similar approach.

2. Literature Review

2.1. Low Carbon Heat scene in Europe

Although more and more European countries are setting decarbonisation goals, in line with the 2050 European Union strategy, heat consumption is still dominated by fossil fuels, as pictured in Fig. 1. More than 30% of energy is consumed in buildings, most of it in the form of heat, and still a large percentage of the buildings in Europe are not retrofitted or have old energy systems. It is estimated that, during the next decades, a drop up to 90% could be achieved in the CO₂ emissions for which the building sector is responsible, if radical energy efficiency measures are applied. (European Commission, 2018)

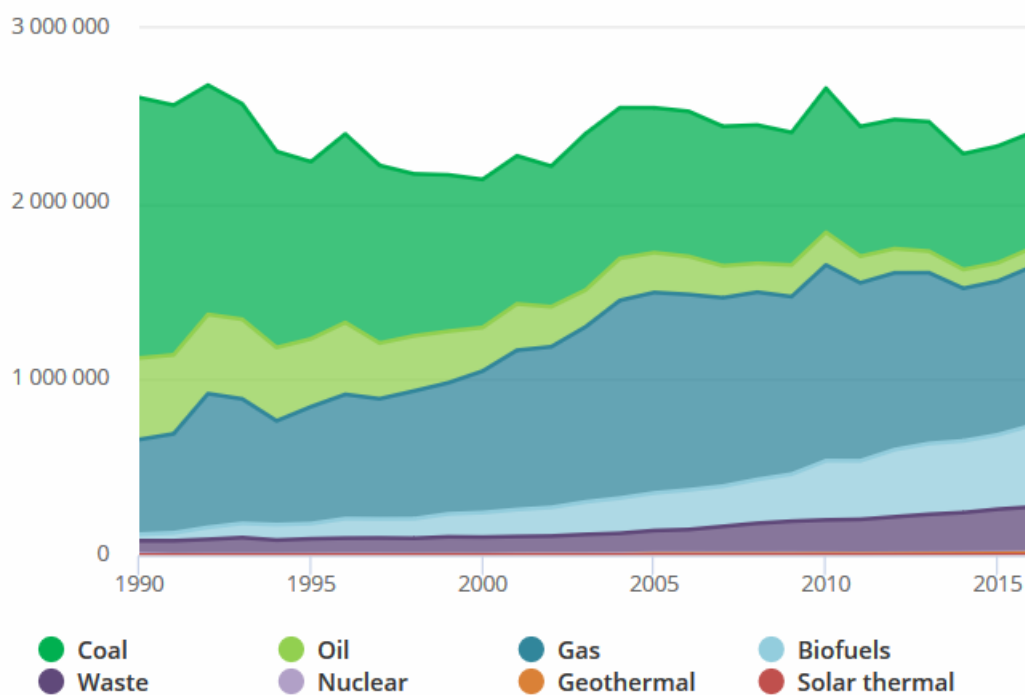


Figure 1. Heat generation in EU-28 by fuel (1990-2016).

Low temperature district heating (DH) in combination with retrofits of existing buildings is considered as one of the key aspects in achieving the goal of carbon-free communities by 2050 (Li, et al., n.d.).

2.1.1. Renewable Energy Systems integration

It is generally accepted that those decarbonisation goals cannot be achieved by a single technology but with a combination of them. However, the most cost efficient and

effective way in which this can be done remains unclear (Anon., 2018) and heavily depends of the conditions and characteristics of each region and application.

2.1.2. The situation in the UK

Currently only 2% of the overall UK heat demand is supplied by DH schemes, with large investments being made mostly in establishing new schemes or refurbishing and expanding already existing ones. Recent findings from an Association of Decentralised Energy 2017 survey (**Fig ()**) reveal that UK DH schemes are –and are expected to remain, judging from the networks currently in the planning or construction stage—dominated by natural gas. (Chauvaud De Rochefort, 2018)

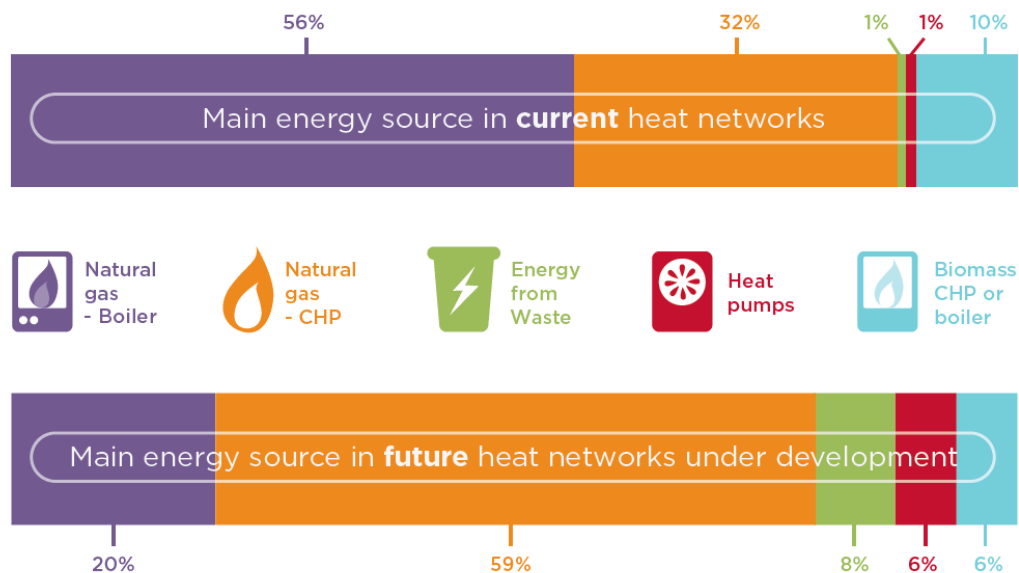


Figure 2. Fuel mix of DH schemes in the UK. (Chauvaud De Rochefort, 2018)

Most of these schemes are large scale and are usually initiated by large construction projects. Since, in most cases, these schemes are supplied by CHP plants powered by gas, the distribution temperatures are high.

Much smaller, community and neighbourhood-scale schemes also exist. An example is the Greenwatt Way sustainable housing development in Slough, England.

3. Technical Background

3.1. Heat Consumption in domestic buildings

Heat is required in domestic buildings both for space heating purposes and for personal use in taps, showers, dishwashers, etc. It is true that comfort levels, that is, the conditions (room temperature, humidity, etc.) under which a person feels comfortable vary, as well as the way in which people consume hot water for their everyday needs. As a result, the occupancy and activity characteristics of each household are of great importance when attempting to design and model the energy system of a building, especially when it comes to models with time steps smaller than 1 hour. They should also be taken into account when simulating the behaviours of larger energy systems, supplying several dwellings, although as the number of consumer rises, their heat demand seems to be smoothened. (Allison, et al., 2018; Baetens & Saelens, 2016)

3.1.1. Domestic Hot Water Consumption

Hot water demand is generally hard to estimate and depends heavily on the number of occupants, their age, and lifestyle. (BRE Housing Centre, 2005) As a result, the mean value of hot water usage (at showers, sinks, etc.), in l/day, can vary significantly from dwelling to dwelling and the patterns of use have to be taken into account, especially when it comes to sizing systems that serve just a small number of dwellings. (Allison, et al., 2018)

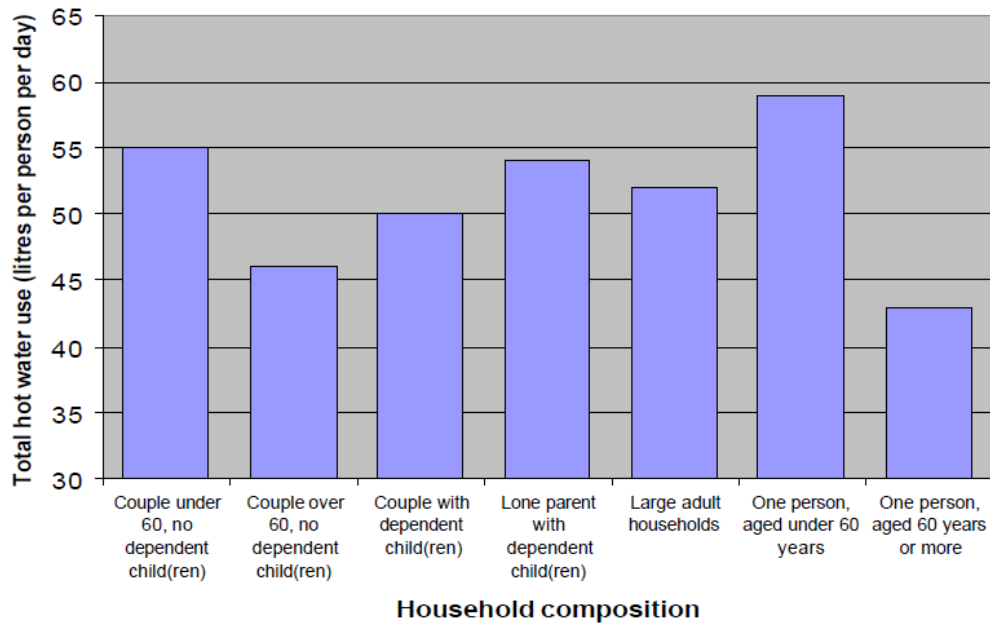


Figure 3. Average daily DHW consumption for typical households of various sizes and compositions. (BRE Housing Centre, 2005)

In 2008, a survey was conducted by the Energy Monitoring Company and the Energy Saving Trust in the UK, aiming to more accurately quantify the volumetric DHW consumption in typical UK dwellings and the respective heat demand for DHW, as well as better understand the patterns of usage throughout the day and examine the water temperature levels at the point of consumption. Measurements were performed on a sample of 120 dwellings with different occupancy characteristics, and equipped with either regular or combi gas boilers. (Energy Monitoring Company & Energy Saving Trust, 2008) Fig. 3 presents the results of the measurements and data analysis regarding the daily DHW volumetric demand of each dwelling, while Eq. 1 was consequently proposed as a way of modelling this demand (in (l/day)) as a function of the number of occupants per dwelling, N , for dwellings where $N \leq 5$:

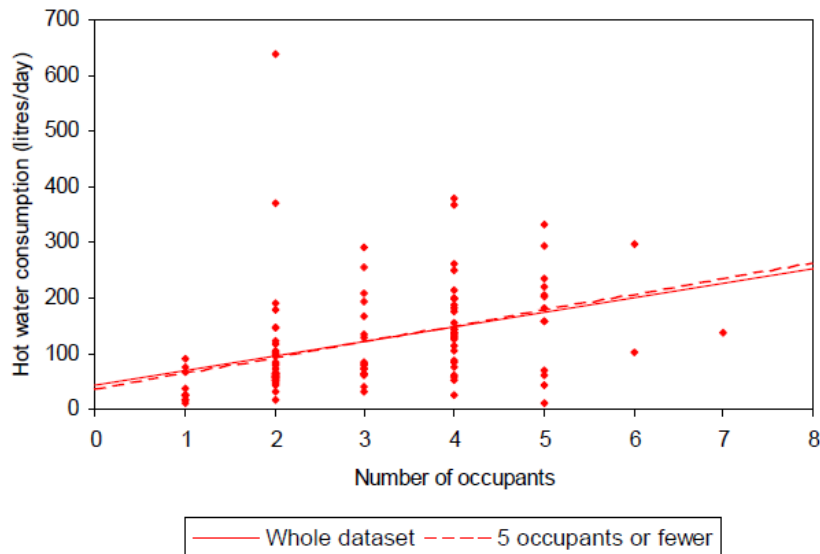


Figure 4 Daily DHW consumption data for UK dwellings ().

$$V_{DHW} = 40 + 28N \quad (1)$$

3.1.2. Energy Consumption for Space Heating

A fast, simplified way of calculating the design heat loss coefficient, H_{Tot} , of a residential building or a smaller “building entity” (i.e. flat, room), based on the bare minimum information regarding building geometry, heat transfer coefficients of individual building elements, ventilation specifics, etc., is provided by BS EN 12831-2:2017. This method is applicable for existing dwellings that are not equipped with mechanical ventilation systems, and takes into account only the thermal losses from the exposed surfaces of the examined building or building entity towards the ambient air and the ground. (BSI Standards, 2017; BSI Standards, 2017) The main steady-state assumptions on which the calculations are based are the following () (BSI Standards, 2017):

- The temperature of the ambient air, the internal temperature of the dwelling, and the ground temperature are constant.
- The physical properties of the building elements are constant. This means that the way in which heat is transferred from the interior to the exterior through walls, windows, roofs, etc., does not vary with time or temperature.
- The resulting heating power is the power needed to maintain the -already heated- rooms of the dwelling under study at the desired temperature.

The Degree Days method can provide a measure of how cold the weather is and account for the variation of the ambient air temperature for a given period of time (e.g. for a day, week, month). This approach is a simplified method for heat energy estimations in buildings that requires minimum data input. The heat demand can be calculated as (Day, 2006):

$$Q_{SH,daily} = H_{Tot} \cdot DD \cdot 24 \quad (2)$$

Where:

DD : the heating Degree Days for a specific day

H_{Tot} : the total (design) heat loss coefficient of the examined building

The accuracy of this method is low, as the internal loads of a building (i.e. heat gains from people, appliances, etc.) are considered through average annual values. Another limitation of using Degree Days for daily calculations arises from the fact that they do not always yield such accurate results for short periods of time, when heat consumption is more severely affected by occupancy behaviours (Anon., 2014).

3.2. Solar Thermal Systems

Solar thermal water systems comprise of solar thermal panels, where the water is heated during days with sufficient sunlight, and a storage tank. Depending on the position of those individual components, they can be classified as thermosyphonic, where the water is stored in a storage tank above the collector(s), or active circulation systems, where the panels can be placed on a roof and the tank at a different location on the ground, so a circulator is needed to pump water through the system. The second systems are what this study will focus on.

Perhaps the most important angles that affect the performance of any solar system are the following (Duffie & Beckman, 2013; Kalogirou, 2014):

- Collector slope or tilt angle, β : it is the angle between the (tilted) surface of a solar collector and the horizontal plane.
- Solar incidence angle, θ : its value changes according to the location where a collector is installed, the day of the year and the time of day.

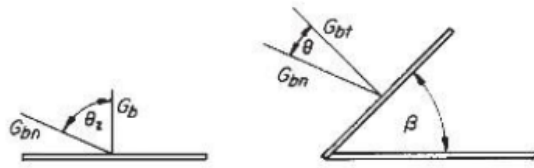


Figure 5. Solar beam radiation on a horizontal surface ($\beta=0$) & on a tilted surface ($\beta>0$). (Duffie & Beckman, 2013)

The standard parameter according to which a solar thermal system is evaluated, both in methods using average monthly data (Kalogirou, 2014) and in more precise methods based on data of higher resolution is the solar fraction. It is generally defined as (Hsieh, et al., 2017):

$$SF = \frac{\text{Heat demand covered by solar supply}}{\text{Total heat demand}} \quad (3)$$

3.2.1. Solar Flat Plate Collectors

Flat plate collectors (FPCs) are simple, low maintenance systems that can be set at a fixed position on a roof or on the ground. They are often used today for medium and low temperature systems. (Quaschnig, 2016)

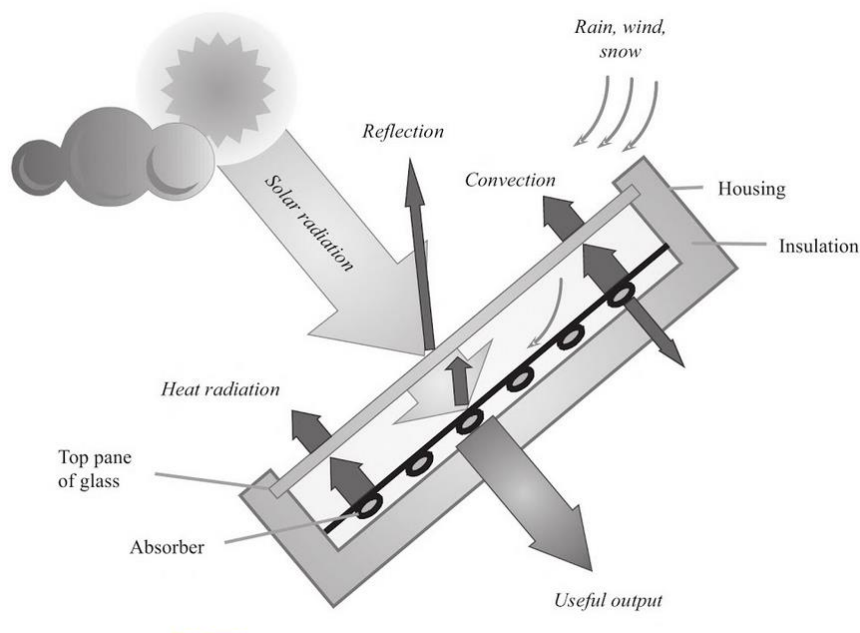


Figure 6. A schematic of the heat transfer procedures between a flat plat collector & its environment. (Quaschnig, 2016)

The useful heat output (in J/s) and the thermal efficiency of the collector under steady-state conditions can be described by the following equations (Kalogirou, 2014):

$$Q_{su} = A_a F_R \cdot [G_t(\tau\alpha)_n - U_L(T_i - T_a)] \quad (4)$$

$$\eta = \frac{Q_{su}}{G_t \cdot A_a} = F_R(\tau\alpha)_n - F_R U_L \left(\frac{T_i - T_a}{G_t} \right) \quad (5)$$

Where:

A_a : the area of the absorber plate, in m^2

F_R : the heat removal factor, defined as $F_R = \frac{(Q_u)_{real}}{(Q_u)_{\tau_{pm}=T_i}}$

$(\tau\alpha)_n$: the transmittance-absorptance factor

U_L : the overall heat transfer coefficient of the collector, in $W/(m^2K)$

G_t : the total solar irradiance, in W/m^2

T_i : the inlet temperature of the fluid medium, in K

T_a : the ambient temperature

Since energy analysis is often conducted on an hourly basis, Q_u can be expressed in joules per hour (J/h), assuming that the temperatures and the absorbed solar energy remain constant over that period. This can be achieved by multiplying the expression in Eq. 4 with a 3600 s/h conversion factor, as Duffie and Beckmann point out. (2013)

By taking into account that the overall heat loss coefficient is a function of the reduced temperature difference between the collector and the ambient air, ΔT , (Eq. 6), the heat output and the efficiency can be expressed as second order polynomials of this temperature difference (Kalogirou, 2014):

$$F_R U_L = c_1 + c_2 \Delta T \quad (6)$$

$$Q_{su} = A_a \cdot [F_R(\tau\alpha)_n G_t - c_1 \Delta T - c_2 \Delta T^2] \cdot \quad (7)$$

$$\eta = F_R(\tau\alpha)_n - c_1 \left(\frac{\Delta T}{G_t} \right) - c_2 \left(\frac{\Delta T^2}{G_t} \right) \quad (8)$$

As for the exact definition of ΔT , Kalogirou highlights that “the standard ISO 9806-1:1994 allows the use of either $(T_i - T_a)$ or $(T_m - T_a)$, where $T_m = (T_i + T_a)/2$ ”. (2014, p. 226)

Quanschning presents a slightly more straightforward way of expressing the thermal efficiency of a flat-plate collector (Eq. 9), by directly using the parameters that result from the steady-state testing as they are presented in the manufacturers’ technical specification sheets. These are the optical efficiency, η_o , which is the efficiency of the collector in the hypothetical case of zero heat losses (in other words, when assuming that $T_m = T_a$), and the heat loss coefficients a_1 and a_2 . (2016)

$$\eta = \eta_o - a_1 \left(\frac{\Delta T}{G_t} \right) - a_2 \left(\frac{\Delta T^2}{G_t} \right) \quad (9)$$

So, by comparing Eqs () and () it becomes apparent that $\eta_o = F_R(\tau\alpha)_n$, $a_1 = c_1$, and $a_2 = c_2$. Some indicative values of these parameters for various solar collectors are presented in Fig. 7.

| Collector type | η_o | a_1 in $W/(m^2 K)$ | a_2 in $W/(m^2 K^2)$ |
|--|----------|----------------------|------------------------|
| Un glazed absorber | 0.91 | 12.0 | 0 |
| Flat-plate collector, single glazing, non-selective absorber | 0.86 | 6.1 | 0.025 |
| Flat-plate collector, single glazing, selective absorber | 0.81 | 3.8 | 0.009 |
| Flat-plate collector, double glazing, selective absorber | 0.73 | 1.7 | 0.016 |
| Evacuated tube collector | 0.80 | 1.1 | 0.008 |

Figure 7. Optical efficiencies and heat loss coefficients of typical solar collectors. (Quaschnig, 2016)

Finally, in order to take into account the actual position of the sun at every hour of the year relative to the position and slope of the solar panel, an additional variable factor, K_θ , is used. The constant, b_o , can be assumed to be $b_o = 0.1$ for FPCs. (Kalogirou, 2014)

$$K_\theta = \frac{(\tau\alpha)}{(\tau\alpha)_n} = 1 - b_o \cdot \left[\frac{1}{\cos(\theta)} - 1 \right] \quad (10)$$

Taking this correction factor into consideration, the equations describing the performance of the FPC for steady-state conditions take their final form (Kalogirou, 2014; Panaras, et al., 2013):

$$Q_{su} = A_a \cdot (\eta_o K_\theta G_t - a_1 \Delta T - a_2 \Delta T^2) \quad (11)$$

$$\eta = \eta_o K_\theta - a_1 \left(\frac{\Delta T}{G_t} \right) - a_2 \left(\frac{\Delta T^2}{G_t} \right) \quad (12)$$

Two popular connection configurations for flat plate collectors are series-in-parallel and parallel. In the case of in-series connection, the input temperature of a collector is equal to the output temperature of its preceding collector, so the calculation becomes more complex.

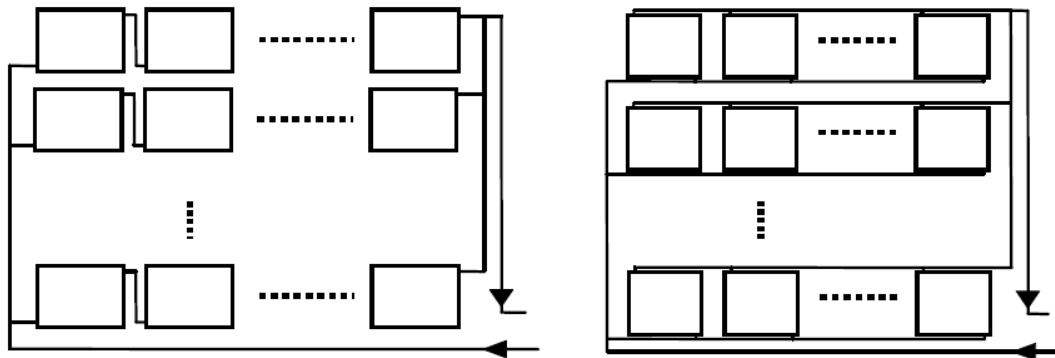


Figure 8. Series-parallel (left) and parallel (right) connection configurations for a field of FPCs (Zelzouli, et al., 2012)

When the flow rate is equal to the ISO 9806-2:1995 test flow rate, no more corrections need to be applied to Eqs. 11 and 12. Otherwise, the thermal output has to be adjusted through a correction factor, K , according to the number of the panels in series. (Kalogirou, 2014) So, in the case of a set of N_s FPCs connected in series, the total output can be modelled as:

$$Q_u = \sum_i^{N_s} A_{a,i} \cdot K \cdot (\eta_o K_\theta G_t - a_1 \Delta T - a_2 \Delta T^2) \quad (13)$$

Where the correction factor is given by:

$$K = \frac{A_c \eta_o}{\dot{m}_s c_{p,s}} \quad (14)$$

3.2.2. Sensible Thermal Energy Storage

Sensible Thermal Energy Storage (STES) systems are systems where the storage medium does not change phase during charging and discharging. These are particularly important in solar heating applications, as one of the main challenges in this case is the low availability of solar energy during the winter months and –in general– during any days of inadequate sunshine throughout the year. The sizing of a STES system largely

depends on the desired time scale of heat storage (daily, weekly, or longer) and the specifications of other auxiliary systems (e.g. boilers, heat pumps) that are often integrated in a heating system, alongside the solar thermal system. (Dinçer & Rosen, 2011)

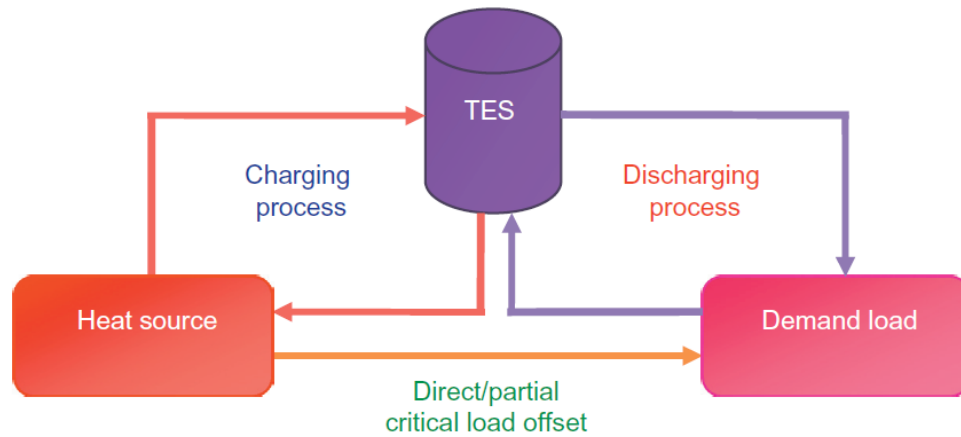


Figure 9. A graphical representation of how a thermal energy system operates as part of a heating system .
(Kalaiselvam, et al., 2014)

Furthermore, the uncertainties and possible lack of data linked to the occupancy and activity patterns of dwellings, as explained in subsection 2.1., can also complicate the sizing of STES systems. Poor estimations of those patterns often lead to the installation of oversized storage tanks, for example, at a high initial cost. (Dinçer & Rosen, 2011)

Short term (i.e. storing heat for up to a few days), sensible storage in WSTs is the simplest and most common thermal storage system, both for building applications and DH schemes. However, storage techniques combining short- and longer-term storage (e.g. with a combination of water tanks at different temperatures and/or borehole storage –that is, storage in boreholes within the ground) are also being investigated and applied for small or community-scale DH schemes based on solar thermal supply systems (Vandermeulen, et al., 2018; Hsieh, et al., 2017).

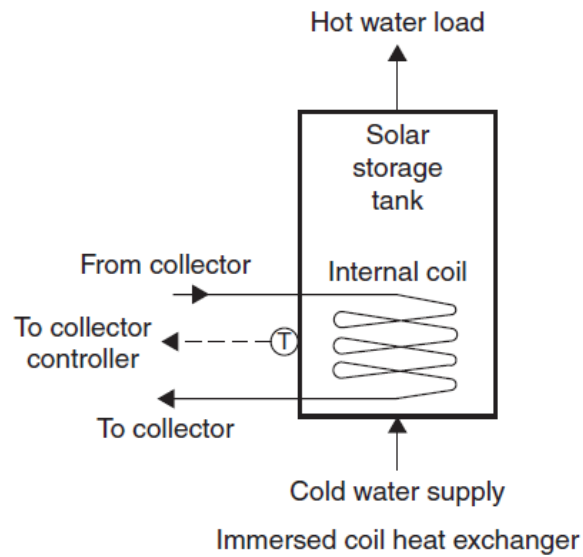


Figure 10. A water storage tank with an immersed solar coil. (Kalogirou, 2014)

A storage tank usually has energy inputs from at least two heat sources, to ensure that there is always enough water at the desired temperature to match the demand of the connected buildings. The transfer of heat between the supply side and the stored water can be done through ‘intermediate’ heat exchangers between the source and the tank, through heat exchangers that are located inside the tank (referred to as “immersed”), or with direct water circulation between the heat source and the tank. (Kleinbach, 1990) Solar thermal systems, especially for small-scale applications, are usually equipped with an internal coil at the bottom of the storage tank, as pictured in Fig. 10 (Kalogirou, 2014).

A WST can be modelled as fully mixed, with a uniform temperature, or as stratified, with layers of water at different temperatures. The degree to which a tank is stratified is determined by the mass and energy flows to and from the tank, as well as from design specifications, mainly the diameter of the inlet/outlet pipes and their position along the vertical axis of the tank. (Duffie & Beckman, 2013)

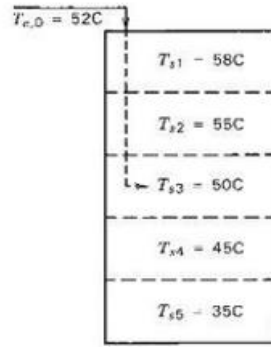


Figure 11. A hypothetical stratified tank with $N=5$ nodes and an inlet flow. (Duffie & Beckman, 2013)

The total storage volume of a vertical, cylindrical storage tank, in m^3 , is given by:

$$V_{st} = \frac{\pi D_{st,i}^2 H_{st,i}}{4} \quad (15)$$

Where $D_{st,i}$ and $H_{st,i}$ are the internal (i.e. inside the external insulation) diameter and height of the tank, respectively.

WST can be modelled in more than one dimensions, involving fluid mechanics, however a 1-D models are preferred when the focus is not on the complex flow mechanisms of the tank. The fundamental assumption on which the 1-D modelling method for stratification is based, is that a temperature gradient of the storage medium exists only along the vertical axis of the tank (Angrisani, et al., 2014).

In other words, the temperature of the storage medium is a function of the vertical distance from the bottom of the tank, h (m): $T = T(h)$. The storage volume of the tank can be split into a number of nodes, N , which are all of equal volume, V_j , and considered to be fully mixed. Each of the nodes is considered as fully mixed, which means that it has a uniform temperature, T_j . (Dinçer & Rosen, 2011). This approach is considered to be suitable and sufficiently accurate for annual simulations of small-scale DH schemes and is presented in Fig. (Hsieh, et al., 2017)

Other general assumptions that can be made in such models are the following (Panaras, et al., 2013; Kleinbach, 1990):

- The density of the storage medium is constant throughout the storage volume.
- The water tank is cylindrical, with a constant cross section, A_c , along its vertical axis, h .

- The water content in the tank is constant regardless of its energy capacity, as every draw-off from the top is replaced by an equal amount of mains water at the bottom node.
- The temperature of the water leaving the tank to satisfy the DHW demand is equal to the maximum temperature of hot water in the tank, $T_{st,out} = T_{st,max} = T_1$, where T_1 : the temperature of the top node.
- The thickness of the external insulation layer is uniform around the tank, so the overall heat transfer coefficient $U_{st} = const$ at any height, h , including the top and bottom surfaces of the tank.
- The effects potential and kinetic energy on the storage medium energy balance, as well as the conduction phenomena between the nodes, are negligible.

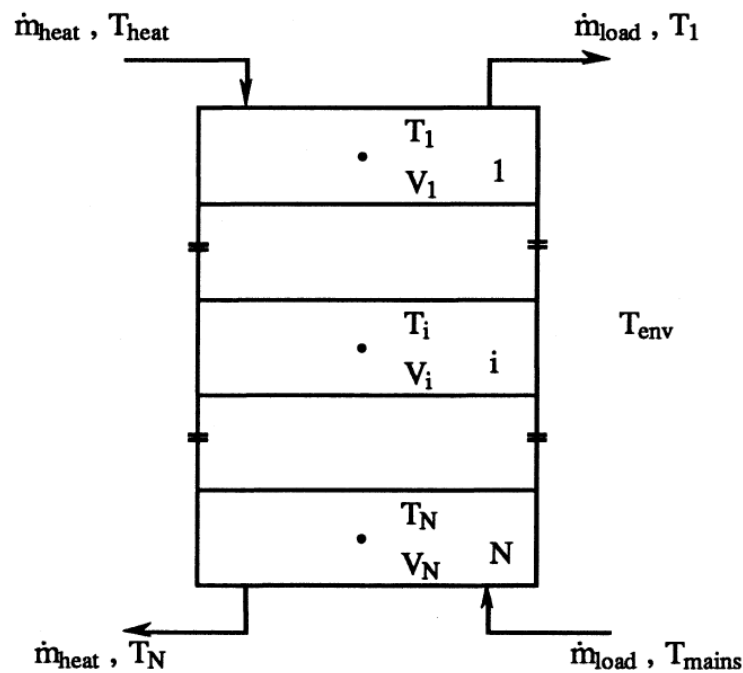


Figure 12. Layout of a nodal model for a stratified water tank. (Kleinbach, 1990)

The left hand side and right hand side of the energy balance equations of each node for a WST that is heated up by a solar coil and a heat pump can be arranged so that the equation that describes the rate of change of the temperature of node j over a time step dt is (Panaras, et al., 2013; Kleinbach, 1990):

$$\frac{dT_j(t)}{dt} = \frac{1}{M_j C_{p,w}} \cdot \left\{ a_j \dot{m}_{hp,t} \cdot c_{p,w} (T_{hp,t} - T_j) + \beta_j \dot{m}_l \cdot c_{p,w} (T_c - T_j) + U_{st} A_{c,j} (T_{env} - T_j) \right. \\ \left. + \dot{Q}_{su} + \begin{cases} \gamma_j \cdot c_{p,w} (T_{j-1} - T_j) \text{ for } (\gamma_j > 0) \\ \gamma_j \cdot c_{p,w} (T_j - T_{j+1}) \text{ for } (\gamma_j < 0) \end{cases} \right\} \quad (16)$$

Where:

$\dot{m}_{hp,t}$: the charging flow rate from a heat pump

\dot{m}_l : the flow rate towards the load

$T_{hp,t}$: the hot water supplied by the heat pump

T_c : the cold water entering at the bottom of the tank

T_{env} : the air temperature in the space where the tank is located

a_j, β_j ,: vectors that describe if a heat pump or load input exists in node j

γ_j : a vector that is calculated by the two aforementioned vectors and represents the mixing the directions of mass transfer in the tank.

A “mixing” algorithm should also be included in each iteration, to ensure that the node temperatures is arranged in such a way that each node has a higher temperature than the one directly below it and a lower temperature than the node directly above it. (Newton, 1995)

The efficiency of a heat exchanger immersed in one or more nodes of the tank --for example, a coil that is part of a FPC circuit- can be approached with the following equation (Panaras, et al., 2013):

$$\varepsilon = \frac{\dot{Q}_{actual}}{\dot{Q}_{max}} \quad (17)$$

Finally, the mean temperature of the stratified tank can be used as a measure of the heat stored in the tank and is calculated by the following equation (Kleinbach, 1990):

$$T_{st,m} = \frac{\sum_{j=1}^N T_j V_j}{V_{st}} \quad (18)$$

Higher (mean) temperatures in the storage tank due to remaining heat that is not utilised by the consumers lead to lower performance of both the solar panels and the heat pump (Panaras, et al., 2013), so this temperature should be monitored and the charging scheme adapted accordingly.

3.3. Air Source Heat Pumps

As with any heat pump, the performance of Air Source Heat Pumps (ASHP) depends on the temperatures between which it operates, and specifically –in heating operation– between the temperature of the heat output, $T_{hp,o}$, and the temperature of the source, $T_{L,o}$. (Reinholdt, et al., 2019)

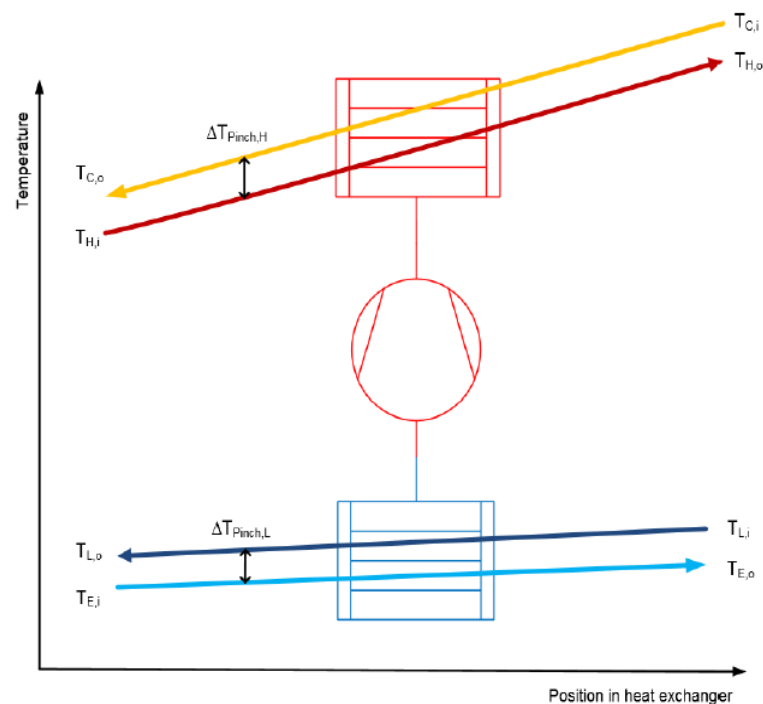


Figure 13. The operation temperatures of a heat pump. (Reinholdt, et al., 2019)

Modern Air Source Heat Pumps can operate at various capacities by adjusting the operation of the refrigerant compressor accordingly. A capacity (or modulation) ratio, r_{mod} , can be calculated, as a measure of the degree of modulation of the heat pump (De Coninck, et al., 2014)

$$r_{mod} = \frac{\dot{Q}_{hp}}{\dot{Q}_{hp,max}} \quad (19)$$

Where $\dot{Q}_{hp} = f(T_{cond}, T_a)$ the thermal output for a certain set of temperatures.

The performance of the ASHP is characterised by its Coefficient of Performance (COP), which is defined as:

$$COP = \frac{\dot{Q}_{hp}}{\dot{P}_{el}} \quad (20)$$

Where \dot{P}_{el} : the electrical input to the ASHP.

It is often deemed useful to express the performance of the heat pump -expressed both by its useful output and its COP- as a function of its characteristic sink and source temperatures. When it comes to the heating operation of an ASHP, these are usually the temperature of the source medium (ambient air) at the input of the evaporator and the temperature of the heating circuit medium (water) at the output of the condenser. Models have been developed in recent years expressing heat pump performance as a function of the difference between these two temperatures. (Kelly & Cockroft, 2011) For heating systems combining a heat pump with a storage tank that is charged by it, it is also convenient to express the output and COP of the heat pump as a function of the temperature of the water stream that leaves the storage and enters the ASHP (Panaras, et al., 2013). Manufacturers usually provide performance data measured under three or four different modulation levels, depending on the type of the ASHP.

3.4. Heat Distribution networks

The diversity factor (DF) of the heat loads is a one of the most representative elements of a DH network, which needs to be calculated and assessed during the early feasibility study stages. (Wiltshire, et al., n.d.) It is always lower at the energy centre, at the starting point of the main distribution pipe, and rises at the points further down the network which are closer to the consumers. The reason for this is that, as the number of consumers supplied by a single pipe drops, the probability of their peak heat demand occurring simultaneously is increased. (Woods, et al., 2015; REHAU, 2013) The DF at a certain point of the DH network can be calculated by the following equation (REHAU, 2013):

$$DF_i = \frac{\dot{Q}_{i,max}}{\sum_j \dot{Q}_{j,max}} \quad (21)$$

Where:

$\dot{Q}_{i,max}$: the maximum heat demand value that occurs at point i , and

$\dot{Q}_{j,max}$: the sum of the peak (nominal) heat demands that occur at connection points j , which are all the points downstream from point i along the network.

The most widely used DF curves, also recommended by the CIBSE UK Code of Practice for Heat Networks, are presented in **Fig ()**. These curves were generated according to Danish, Swedish and German standards. It should be noted that they were based on a certain type of “normal” dwelling, with specific assumptions made for its occupancy and hot water consumption patterns, so they do not exactly fit every possible neighbourhood mix of dwelling types and heat consumer behaviours. The Danish standard DS 439, specifically, is recommended by UK codes of practice as a set of reliable guidelines for performing DH feasibility studies (Woods, et al., 2015).

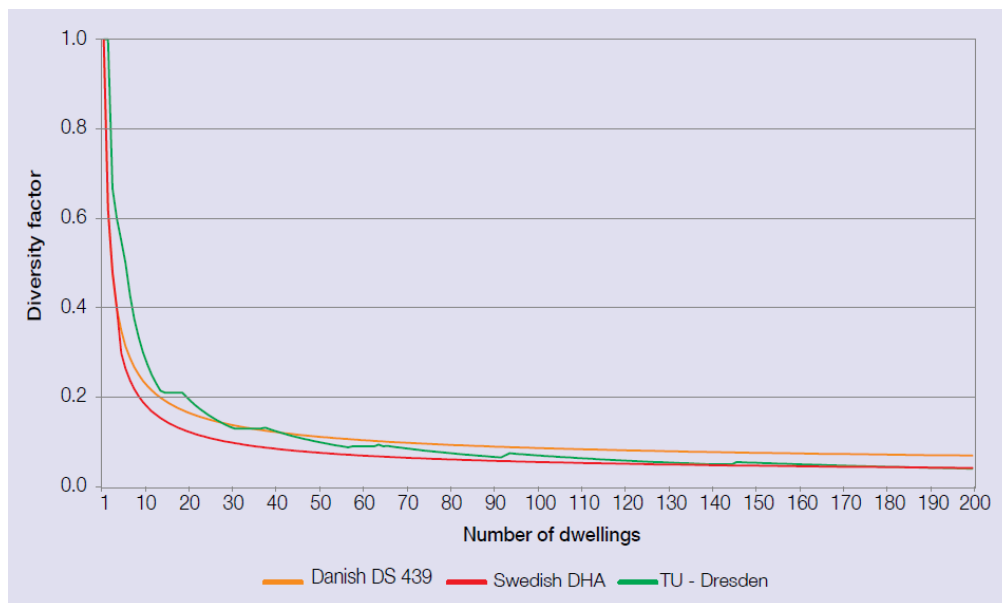


Figure 14. Commonly used diversity factor curves for heat networks. ()

The supply and return pipes used in DH networks of medium or low temperatures are either encased in the same insulation (twin pipes) or have separate insulations around them (singly pipes), as pictured in Fig . The flow pipe is indicated with red colour and the return pipe with blue.

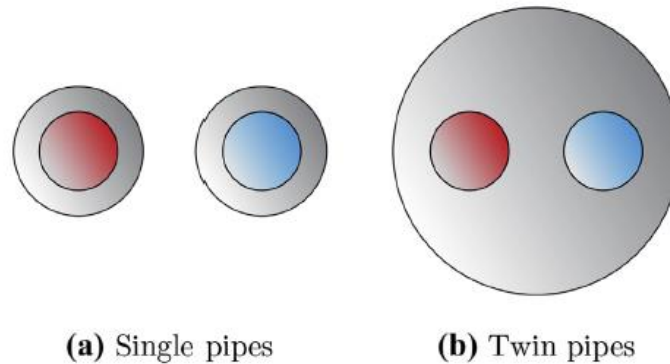


Figure 15. A schematic of single (left) & twin (right) DH pipes.. (van der Heijde, et al., 2017)

The heat losses along the network depend on (Østergaard & Andersen, 2016; Wallentén, 1991):

- The size and length of the pipes
- The level of insulation around the pipes
- The operational temperatures and the ground temperature

Additionally, according to van der Heijde, et al., (2017) heat losses appear to be independent of the water flow rate in the pipes. As for the operational temperatures, they can be considered as fixed or variable -as does the flow rate that supplies the network. They are usually assumed to be fixed, especially in high level analysis or feasibility studies. Then, the total supply mass flow rate can be calculated by the following equation, dividing the total demand with the target temperature difference at the side of the consumers (Østergaard & Andersen, 2016):

$$\dot{m}_{tot} = \frac{\sum \dot{Q}_{i,max}}{\Delta T_{i-o,c}} \quad (22)$$

The dependence of the heat losses on the aforementioned temperatures can be modelled in steady-state conditions by the average operational temperature (van der Heijde, et al., 2017; Østergaard & Andersen, 2016):

$$T_m = \frac{T_{p,o} + T_{p,i}}{2} - T_g \quad (23)$$

This methodology can provide an estimate of the average heat losses from the network over a certain period of time, assuming that the operating temperatures remain constant throughout that period.

4. Method

4.1. Assessing Heat Demand in Domestic Buildings

4.1.1. Domestic Hot Water Demand Analysis

In order to generate DHW demand profiles for each of the dwellings considered for the study, DHWCalc, a free tool developed by the University of Kassel, can be used. The tool is able to generate demand profiles with time step sizes ranging from 1min to 1h, based on a mean daily demand value (in l/day), time-of-use patterns throughout weekdays and weekends, and holiday periods with accordingly modified DHW use, which can all be specified by the user (Jordan, et al., 2017).

DHWCalc can consider up to 4 different draw-off load cases, representing the different ways in which hot water is usually used in dwellings: short (e.g. use of tap water in sinks), medium (e.g. dishwasher), shower, and bath (Jordan & Vajen, 2001). Realistic assumptions are made by default by the tool regarding the volumetric flow rate and duration of each of those draw-offs. These assumptions were also used for the current study and are presented in Table 1.

Table 1. Draw-off categories and their respective mean flow rates, standard deviation, and time durations().

| | V_m (l/min) | σ (l/min) | t_d (min) |
|--------|---------------|------------------|-------------|
| Short | 1 | 2 | 1 |
| Medium | 6 | 2 | 1 |
| Shower | 8 | 2 | 5 |
| Bath | 14 | 2 | 10 |

Furthermore, different daily usage patterns and holiday periods throughout the year were assumed for each dwelling, to provide a more realistic case of how DHW consumption behaviour differs between users. Since total annual DHW consumption data was available for the dwellings of the case study, a simple mean average for the daily DHW demand (in l/day) of each dwelling was calculated and used as input for the DHW calculations, having excluded the holiday periods (during which DHW demand was set as zero) from the total days of occupancy. As can be seen in Table 1, almost all of the resulting mean daily DHW demand values fall within the 40 to 50 l/day range, in agreement with the results of the EFUS Survey that was mentioned before, but much lower than the more recent BRE survey.

The hourly profiles can provide representative, average flow rate values for each hour of use, which, when summed over the entire year, lead to the annual DHW consumption value.

4.1.2. Space Heating Demand Analysis

Hourly metered data can be used to convert the daily profiles calculated using the Degree Days method into hourly. The average internal heat gains and solar gains were not considered necessary for the purpose of this study, as the focus here is not on building simulation and the generated profiles would anyway be scaled according to the measured SH demand for the buildings of the Case Study. The Degree Days of the simulation year can be used to produce a scaling factor that adjust the timeseries of metered data to the weather conditions of the simulated year.

In accordance with recent studies (Allison, et al., 2018), an activity profile of 07:00-23:00 maximum duration can be assumed. In other words, it can be assumed that there is no SH demand during the night.

4.2. Heating System Modelling Approach

The MATLAB programming environment is frequently used to set up energy analysis and optimisation algorithms for building or district level schemes that combine renewable and conventional energy resources. (Panaras, et al., 2013; Carpaneto, et al., 2015) Its flexibility and speed is the reason why it was employed in this study for the modelling of the supply side of the DH scheme.

The chosen design variables investigated were the size of the WST and the capacity of the ASHP. The main general assumptions applied across the model were the following:

- Water is considered as an ideal liquid, with $\rho=\text{const}$, $c_p=\text{const}$ for the examined range of temperatures.
- Flow rates at the supply side were constant, and the only variable flow rates are those of the SH and DHW supply

The main programme reads the following inputs data from MS Excel files (as hourly timeseries for an entire year):

- Local ambient conditions (ambient temperature, solar irradiation at the level of the ground)
- Heat demand data for SH and DHW for the buildings under study (in kW and L/h, respectively)
- Night charging schedule (as a boolean matrix)
- Cold water temperature, varying monthly (for the input at the bottom of the storage tank)

4.2.1. Solar Collector Model

The “Solar” function was set up in the MATLAB environment, and linked to the “Main” programme, based on the following modelling assumptions:

- The collectors are single glazed, selective FPCs, and identical to each other. All of them have the same orientation (South, 0°) and tilt angle. Both of these angles remain constant, as they are not included in the design variables of this study.
- There is a number of collectors, N_s , connected in series, while several different series of collectors, N_p , can be linked to each other in parallel configuration. In order to avoid overcomplicating the model, the temperature drop that occurs as the working fluid flows between two consecutive FPCs is not taken into account. Instead, the collectors in-series are modelled as a single collector with an absorber area equal to the sum of their absorber areas, according to Eq. 11.
- The flow rate of the water-antifreeze mixture is the same for each collector –as they are identical- and is considered constant throughout the simulation. The total flow rate of all the series of FPCs, through which heat is transferred to the stored water, is equal to the sum of the flow rates of each series.
- Potential heat losses from the pipes connecting the collectors to the tank are not taken into consideration.

The properties of the chosen collector, based on the ISO 9806-1:1994 test and provided by the manufacturer, are included in the “Solar” function as parameters. As for the incidence angle modifier, it is calculated in a separate MS Excel spreadsheet, according to the location (coordinates) of the system under study and the chosen position angles, and then passed on to the function as an input. The function calculates the mass flow

rate within the collector based on the flow rate used during the ISO 9806-1:1994 steady-state test, which is equal to $0.02 \cdot \dot{m}_s$. The thermal output, \dot{Q}_{sol} (in W), and efficiency of a single series of N_s FPCs are calculated by applying Eq. 11 and 12 respectively, for $\Delta T = T_i - T_a$.

4.2.2. Thermal Energy Storage Model

The choice was made to examine the storage tank under study as a stratified tank, in an attempt to more accurately model the effect of having more than one sources supplying heat at different heights of the tank. The simplifications already mentioned at the previous chapter were made, and a model with $N=3$ nodes was set up on MATLAB as a separate function.

Designated vectors in the function indicate the placement of water inlet/outlets and heat inputs in the tank, as shown in the energy balance equation Eq.16.

The top node, $j=1$, receives the water input from the ASHP, while from this node the water flow that covers that DHW demand of the connected buildings leaves the tank.

The middle node, $j=2$, includes the output of water flow, $m_{hp,t}$, which returns to the ASHP.

Finally, node $j=3$, at the bottom of the tank, is charged by the solar FPC system through an immersed coil heat exchanger. Furthermore, this node receives a cold water mass flow input from the bottom of the tank.

Since performing heat transfer analysis on a heat exchanger level is out of the scope of this study, the heat passed from the immersed heat exchanger of the solar circuit to the water stored at the tank is reduced by the efficiency factor, ε_{sol} , before being passed on as an input in the “Storage” function.

For a 3-node stratification tank, Eq.16 can be used to describe the energy balance in each node. When all factors are arranged so that the rate of temperature change of node j is presented as a function of the temperatures of all the nodes, the result is a linear system of three differential equations:

$$T' = A \cdot T + d \Rightarrow$$

$$\begin{pmatrix} \frac{dT_1(t)}{dt} \\ \frac{dT_2(t)}{dt} \\ \frac{dT_3(t)}{dt} \end{pmatrix} = \begin{bmatrix} b_1 & c_1 & 0 \\ a_1 & b_2 & c_2 \\ 0 & a_1 & b_3 \end{bmatrix} \cdot \begin{pmatrix} T_1(t) \\ T_2(t) \\ T_3(t) \end{pmatrix} + \begin{bmatrix} d_1 \\ d_2 \\ d_3 \end{bmatrix} \quad (24)$$

For the purpose of this study, the Crank-Nicolson method was employed in order to solve the system numerically, as suggested by (Newton, 1995), At the end of each iteration within the Crank-Nicolson method loop in the “Storage” function, the nodes are rearranged according to their temperature, from the warmest to the coldest one. The algorithm is set to end when a difference smaller than 0.03°C is achieved between two consecutive iterations.

$$\begin{aligned} \text{Type } equa T_{new,j}(t) \\ &= T_j(t) + dt \\ &\cdot \left[\frac{a_j}{2} (T_{j-1} + T_{new,j-1}) + \frac{b_j}{2} (T_j + T_{new,j}) \right. \\ &\quad \left. + \frac{b_j}{2} (T_{j+1} + T_{new,j+1}) + d_j \right] \end{aligned} \quad (25)$$

The time step here can be shorter than that of the rest of the model, in order to capture the heat transfer phenomena within the tank more accurately and provide a more realistic approximation of the average node temperatures at each time step. However, since the rest of the models in this study consider steady-state conditions and do not take variations over short periods of time into consideration, the time step was set at 1 hour.

Moreover, several basic assumptions and simplifications were made while setting up the storage tank model:

- The water input at the bottom node of the tank has a temperature that is equal to the average temperature of the water mains and the return temperature from the DHW circuit at the point of the energy centre:

$$T_c = \frac{T_{mains} + T_{DHW,i,p}}{2}$$

- The tank is placed in the energy centre, whose envelope is insulated in such a way that the temperature at its interior, T_{ec} , generally remains constant and only varies between the warm and cold months of the year so that:

$$T_{ec} = \begin{cases} 18^{\circ}\text{C}, & \text{from May until September} \\ 15^{\circ}\text{C}, & \text{for the rest of the year} \end{cases}$$

4.2.3. Heat Pump Model

For the specific system configuration investigated here, since the heat pump is the only supply system covering the SH demand and has no access to storage, the capacity of the selected heat pump should be enough to cover the total SH demand and distribution losses during the coldest day of the year.

While attempting model the performance of the ASHP, Fig. was put together was put together using performance data available for a Mitsubishi ASHP for the temperature range of interest for this application described later in this thesis.

This heat pump can only operate at medium and maximum capacity levels and ambient temperatures above zero for $T_{hp,o}=60^{\circ}\text{C}$. Furthermore, for the chosen temperature ranges, the heat pump achieves its highest COP for $T_a>10^{\circ}\text{C}$ and $T_{hp,o}=45^{\circ}\text{C}$. This can be explained by the fact that the temperature lift is smaller under these conditions.

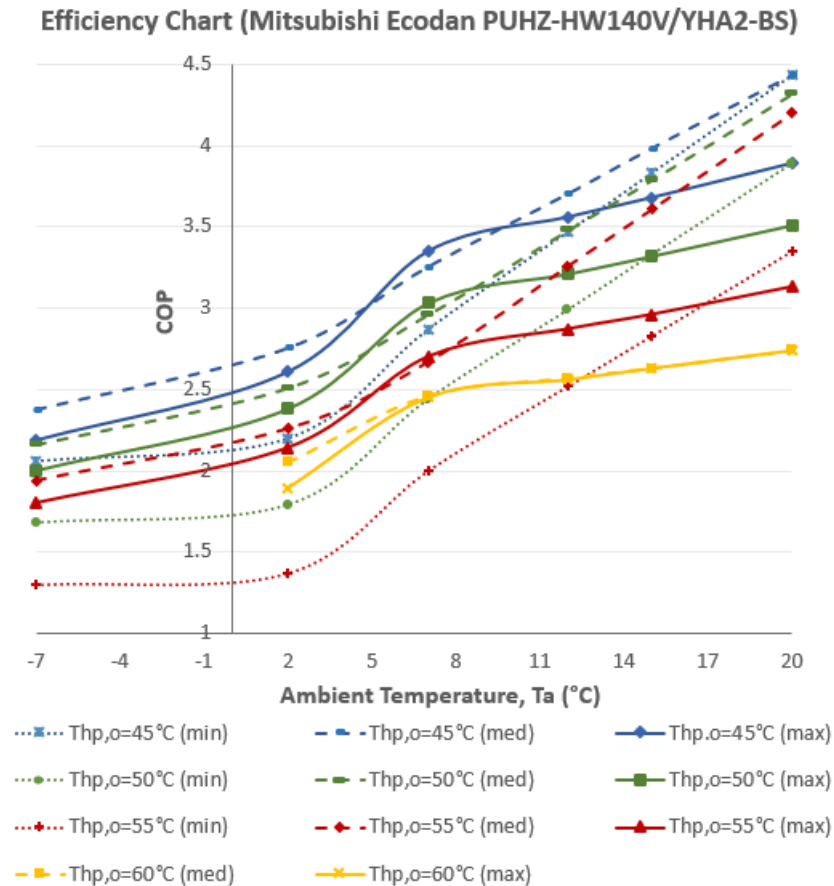


Figure 16. The COP of the chosen heat pump for the baseline scenario as a function of the ambient air and output water temperatures.

Perhaps the most useful conclusion that resulted from this performance map was that the ASHP behaves in a similar way while operating at a single capacity level and different temperatures. Consequently, ASHP performance could be mapped in 3-D by fitting the given measured data into two surfaces, one for the thermal output, $Q_{th}=f(Thp,o,Ta)$, and one for the performance coefficient, $COP=f(Thp,o,Ta)$. In this way, Q_{th} and COP can be easily calculated for any given (Thp,o, Ta) operation point.

Fitting the data for each capacity level in a surface was done by using the Curve Fitting application on MATLAB. This tool allows the user to try out different surface fits, while also providing an evaluation of each fit through a regression analysis. In the case of polynomial fits, the surface can be a function of various degrees of the two independent variables.

For this study, the HP Q_{th} and COP were expressed as a second degree function of Thp,o and third degree function of Ta , as this led to a better overall fit to the set of datapoints provided by the manufacturer. The coefficients resulting from this fit can be

entered in the “Heat Pump” function as parameters, and the known demand and temperatures at every time step as inputs. The calculated ASHP output is always equal to the demand and, according to this value, the nearest possible COP is calculated using the curve coefficients and given temperatures.

As there is no data available by the manufacturers regarding the effect of the inlet temperature at the condenser on the performance of the heat pump, this temperature could not be included in the generation of the characteristic surfaces.

4.2.4. District Heating Network

A simple way of sizing a piping network is by using the MS Excel spreadsheets or online tools of pipe manufacturers. These tools take the operating temperatures, as well as the insulation properties of different products and of different diameters -at these temperatures- into consideration. Such an approach was also taken for this study, using piping properties by REHAU. (REHAU, 2013)

4.2.5. Supply – Demand Matching

Ideally, for the demand for SH and DHW to be covered solely by the solar system and the heat pump, the thermal output of the heat pump should be equal to amount of heat required to cover the space heating load of the connected buildings, $Q_{SH,tot}$, and the heat input required in the upper nodes of the storage tank, $Q_{st,charge}$, for the stored water to reach the desired output temperature:

$$Q_{hp,th} = Q_{SH,tot} + Q_{st,charge}$$

However, this might not always be the case. Generally speaking, depending on the specifications of the chosen heat pump, the heat demand of the connected buildings might occasionally be higher than that which the heat pump can provide for the given operational temperatures. For this reason, a check is made within the “Heat Pump” MATLAB function and the thermal output adjusted to the maximum available output for the given temperatures, if the demand exceeds it. A heat loss factor (LF) is also included as a parameter, to take into consideration the distribution heat losses while calculating the needed output of the ASHP.

The lower electricity tariff applied from midnight until early each morning, which has been mentioned in the previous chapter, is a great financial incentive for charging the storage tank through the heat pump during those hours. The carbon intensity of the UK grid also tends to decline and reach its minimum daily values around that period, which means that the electrical energy consumed then has a lower environmental impact. The charging strategy applied in this study is explained below.

Two cases of “renewable” charging of the storage tank are considered:

1. Tank charged by the ASHP during night time (00:00 – 07:00 daily):

This approach is in agreement with the domestic activity profiles adopted in other relevant studies (Allison, et al., 2018), so it can be safely assumed that there is no SH demand during that period. Consequently, if the ASHP is turned on, it will be solely to charge the tank, and not to supply water to the SH network as well. This means that water will circulate only in the loop that connects the ASHP with the top and middle nodes of the storage tank.

As suggested by the investigation of a similar DHW system that the current study was heavily based on (Panaras, et al., 2013), the ASHP is activated when the temperature in the middle node, $j=2$, drops below a $T_{2,set} = 52^{\circ}\text{C}$ setpoint.

2. Tank charged by the solar system during day time (when available):

During the 07:00 – 23:00 period every day, the tank is charged by the FPCs when both of the following conditions are true:

- The global incident solar radiation on the panels has a positive value
- The temperature difference between the output temperature of the panels and the middle of the tank is $\geq 5^{\circ}\text{C}$ –this is an activation condition that was also adopted by Panaras et al. (2013).

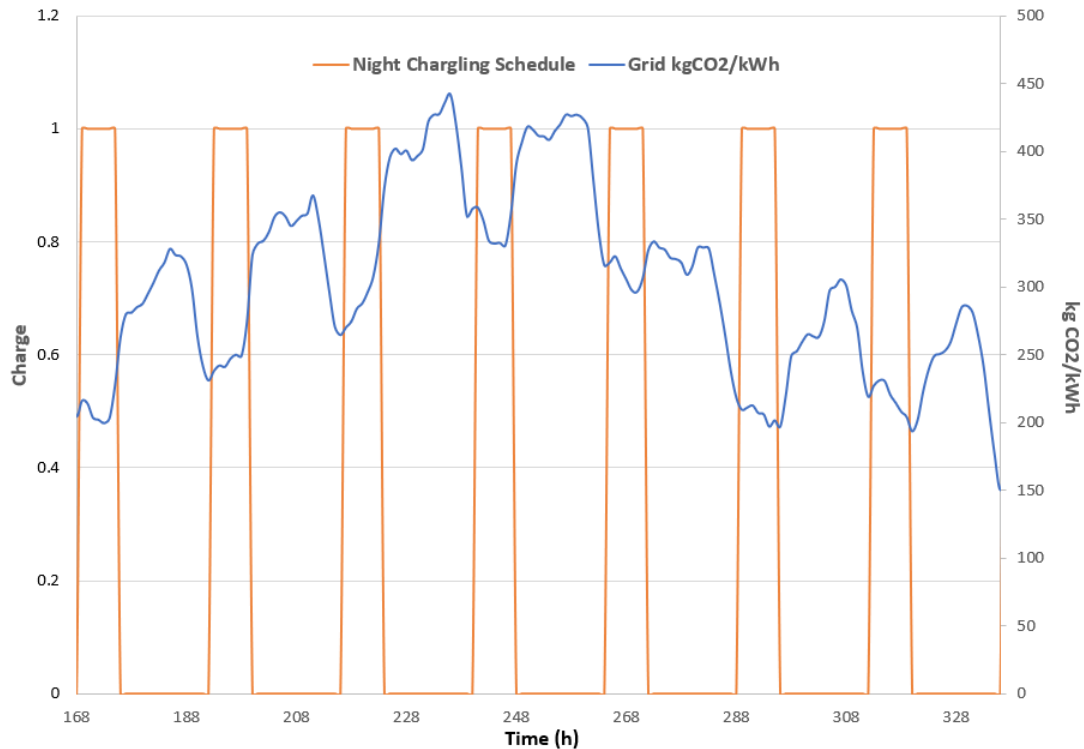


Figure 17. Charging schedule vs Grid carbon intensity for 2 weeks in January.

Fig is provided as an example of how the overnight, low-tariff charging schedule by the ASHP coincides with the time when UK grid electricity is “cleaner”. The storage can be charged by the ASHP when Charge = 1.

The aforementioned assumption that the ASHP can either supply the SH or the ST charging circuit, and never both at once, was made in order to disengage the two operations and the mass flows of each circuit, thus simplifying the model. It should also be repeated here that a higher charging temperature of 60°C was not attempted, due to the fact that the chosen ASHP on which the model was based cannot provide this output temperature when external temperatures approach or drop below zero.

4.3. Assessing Costs & CO₂ Emissions

The operational cost of the ASHP in this model can be assessed by calculating the needed electrical input, with Eq.20, and multiplying it with the costs of import from the electrical grid.

As for the respective CO₂ emissions from the ASHP, in recent years a programming interface has been developed in the UK that provides quite accurate forecast of the “carbon intensity” –in other words, the CO₂ emissions per generated kWh of electricity– of the UK electrical grid. This forecast is based on historical data by most

UK-based electricity plants, provided that their generation is metered, and considers the different sources of energy (natural gas, wind, biomass, etc.) in the electricity mix, as well as the losses while this energy is being transmitted and distributed across the country. This data is available online and the public is encouraged to shift their energy use according to this forecast. (National Grid, et al., n.d.). The classification of the grid's intensity is provided in Fig () below:

| Index | gCO₂/kWh | | |
|--------------|----------------------------|-------------|-------------|
| | Carbon Intensity | | |
| | 2017 | 2018 | 2019 |
| Very High | 400+ | 380+ | 360+ |
| High | 300-399 | 280-379 | 260-359 |
| Moderate | 200-299 | 180-279 | 160-259 |
| Low | 100-199 | 80-179 | 60-159 |
| Very Low | 0-99 | 0-79 | 0-59 |

Figure 18. Classification of UK grid carbon intensity in several categories for the years 2017-2019. ()

Although, naturally, there are forecast errors in this methodology, it is considered as accurate enough indication of the CO₂ emissions linked to grid electricity use, for the scope of this study.

5. Case Study: Findhorn Ecovillage

Findhorn Ecovillage is a sustainable community at Northeast Scotland. Its residents are highly environmentally conscious, promoting environmental education and a life with a low ecological footprint. The domestic and community buildings in the area are built to high efficiency standards. Furthermore, the community owns four wind turbines of a total 750kW capacity and its own distribution network, managed by the Findhorn Foundation.



Figure 19. A panoramic view of Findhorn Ecovillage. (Ecovillage Findhorn, n.d.)

For the purpose of this project, a small number of efficient buildings located at the Ecovillage and served by a small DH scheme, which includes solar thermal panels and an ASHP, were considered as a case study. Hourly weather data for Findhorn (57.6591,-3.6107) were obtained from the global MERRA-2 reanalysis database through the Renewables Ninja website. This was preferred over the other database because more recent data was available (from 2014 onwards). Aerosol observations and cloud cover were taken into account in generating the solar irradiance data (Pfenninger & Staffell, 2016), so these datasets are considered as an accurate input for realistic calculations of solar thermal output.

5.1. Examined Buildings

The cluster of dwellings under study consists of four detached and semi-detached buildings, with one or two flats per building. The dwellings' floor areas are all below 40m² and they include just one bedroom, so, presumably, there are up to two occupants per dwelling.

Table 2. Geometrical specifications of the existing buildings of the Case Study.

| Dwelling No | Dwelling Type | Floor Area (m²) | Ext. Walls Area (m²) |
|--------------------|-------------------------|---------------------------------------|--|
| 1 | End of terrace bungalow | 37.52 | 60.77 |
| 2a | Ground floor flat | 38.58 | 44.03 |
| 2b | 1st floor flat | 38.58 | 64.29 |
| 3a | Ground floor flat | 38.58 | 44.03 |
| 3b | 1st floor flat | 38.58 | 64.29 |
| 4 | End of terrace bungalow | 37.52 | 60.77 |

The information about the buildings' geometrical characteristics (floor, external wall, glazing areas, etc.) used in this study were taken from architectural drawings of the development which were shared with the Energy Research Systems Unit at the University of Strathclyde.

5.2. Examined Heating Scheme

The main energy sources of the existing heating scheme are two arrays of three solar thermal panels (FPCs) each, connected in series, for the DHW needs of the buildings, and an ASHP that supplies hot water for SH purposes.

There are two sets of three in-series FPCs mounted on the roofs of the two-storey buildings. Those sets are connected in parallel, which means that the mass flow rate entering the tank from the FPCs is equal to the sum of the flow rates in each individual FPC.

Furthermore, water is stored in a 550l vertical tank WST, to be used the DHW network. The tank is located in the energy centre (EC), very close to the buildings and the ASHP. The lower part of the storage is charged by the FPCs through an immersed solar coil. The ASHP is also utilised in order charge the storage when needed, so that the desired temperatures are achieved. Since the DHW seems to be supplied directly to the taps of the consumers through this configuration, a direct electric heater is also included at the bottom of the tank, to heat up the stored water at 60°C to eliminate the risk of Legionella.

Each building is equipped with a Substation (SS), which links it to the EC through separate pipes for SH and DHW.

5.3. Cost of electricity

It is assumed that a night and day tariff are applied to grid electricity import at Findhorn, according to the Economy 7 tariff. (Scottish Government, 2015)The night tariff is lower, and applicable from 12am till 7am. It is assumed to be equal to 11.087p/kWh. The day tariff applies for the rest of the day and is assumed equal to 13.762p/kWh for this study.

The locally generated electricity from the community-owned wind farm has not been taken into consideration.

6. Simulated Scenarios

Different scenarios were investigated using the analysis and modelling methodology presented in Chapter 4. The “Baseline Scenario” was heavily based on the existing system and buildings, with slight modifications. The rest of the scenarios explored the possibility of expanding and scaling up the system in order to include neighbouring buildings, as well as the possibility of having identical, separate systems, which would supply neighbouring buildings in Findhorn Ecovillage.

The U-values used for the external structural elements of the buildings are either the ones provided by the existing buildings’ Energy Performance Certificates, or assumed, and are presented in **Table** .

Table 3. U-values of the building envelopes.

| Building Element | U (W/(m²K)) |
|-------------------------|-------------------------------|
| External walls | 0.17 |
| Windows | 1.20 |
| Roofs | 0.14 |
| Floors | 0.13 |

A first estimation of each dwelling’s overall heat loss coefficient, H_{tot} , and design load, H_{Tot} , was performed on MS Excel for the given building geometry and thermal properties specifications, using the simplified calculation method in accordance with BS EN 12831-2:2017. Those values were later corrected, in order to match the peaks of the generated SH demand profiles.

Since metered annual consumption data were available for 2018, the Degree Days method was used to generate daily demand profiles for the same year. The heating degree days for each day of 2018 from the weather station closest to Findhorn Ecovillage, Kinloss Weather Station (3.56W, 57.65N), which are available for download online (BizEE Weather Data for Energy Professionals, n.d.), were used. In order to generate the data, the base temperature was set to 15.5C, which is the balance

temperature for heat demand calculations in the UK (Day, 2006). Furthermore, the following design temperatures were considered:

- Average ambient temperature = 8.2°C for Findhorn (Climate-Data.org, n.d.)
- Base design temperature = 4°C, as recommended by Watkins 2011 for exposed houses in coastal UK areas.

The performance parameters for the chosen solar collectors, which are the same as those of the existing system, were $a_1 = 4.021 \text{ W/m}^2\text{K}$, $a_2 = 0.022 \text{ W/m}^2\text{K}^2$, $\eta_o = 0.781$, for FPCs with $A_a = 2.3\text{m}^2$ (AES Solar, n.d.).

The incidence angle modifier, K_θ , was calculated on MS Excel, applying the needed solar time corrections, for the coordinates of Findhorn and assuming $\beta=57^\circ$. An 80% v/v concentration antifreeze-water mixture was assumed as the working fluid of the FPC circuit. For the type of antifreeze recommended by the FPC manufacturer and the operational temperatures of the system, the mixture's average specific heat capacity was considered to be $c_p = 2.780 \text{ kJ/kgK}$ and constant for the entire temperature range.

As for the useful heat transferred by the immersed solar coil to the bottom node of the storage tank, an efficiency factor $\varepsilon_{sol} = 0.7$ was assumed, in accordance with the experimentally determined efficiency factor by Panaras et al. (2013).

The dimensions of the water tanks were based on a UK manufacturer's technical datasheets for stratification tanks with at least one hot water flow input and a single, immersed heat exchanger coil at the bottom of the tank. () As for each tank's insulation properties, an external insulation thickness of 100mm and an overall heat transfer coefficient $U_{st} = 0.45 \text{ W/m}^2\text{K}$, uniform around the tank, were assumed and kept constant for all scenarios. The charging strategy applied for the simulations of the different scenarios is the one proposed in Chapter 4. The supply temperature was kept at 55°C for the DHW because this is the highest available temperature that this ASHP can over for the entire T_a temperature range. It is assumed that it supplies the dwellings through a direct heat exchanger unit, so it doesn't involve any legionella danger.

Finally, after converting the DHW volumetric flow demand profiles into DHW heat demand profiles (i.e. average kWh/h), it was observed that the maximum loads for DHW –per dwelling– were at most twice as high as those that resulted from the SH

demand analysis, while the total load was slightly lower than that of for SH. As a result, and in agreement with the specifications available for the existing system of the Case Study, distribution pipe dimensions (diameters and lengths) between the EC and each building's SS were considered to be the same for both the SH and the DHW network. Since the operating temperature ranges for both networks were roughly the same, as well, and according to the methodology presented in Chapter 4, the heat losses were also assumed to be the same for both networks. Those were calculated for pipe dimensions and properties of REHAU.

6.1. Baseline Scenario

In the Baseline Scenario, the buildings on the demand side are the existing buildings as described in the Case Study. The Degree Day method as well as “generic” hourly SH demand profiles which resulted from past research at the Energy Research Systems Unit (ESRU) at the University of Strathclyde were used to generate the SH profiles.

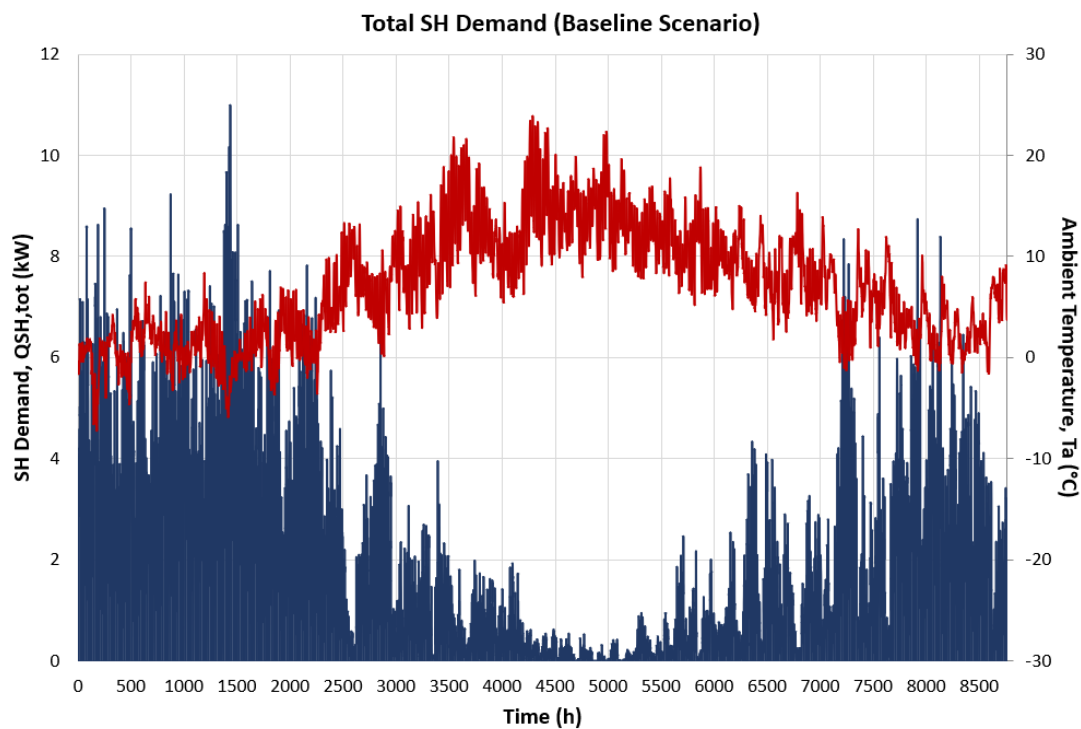


Figure 20. Baseline Scenario total SH demand.

The different heat use patterns for each flat, resulting from the various generic profiles and time-of-use assumptions the analysis was based on, can be clearly seen in **Fig** for the first week of February, with external temperatures, T_a , near zero.

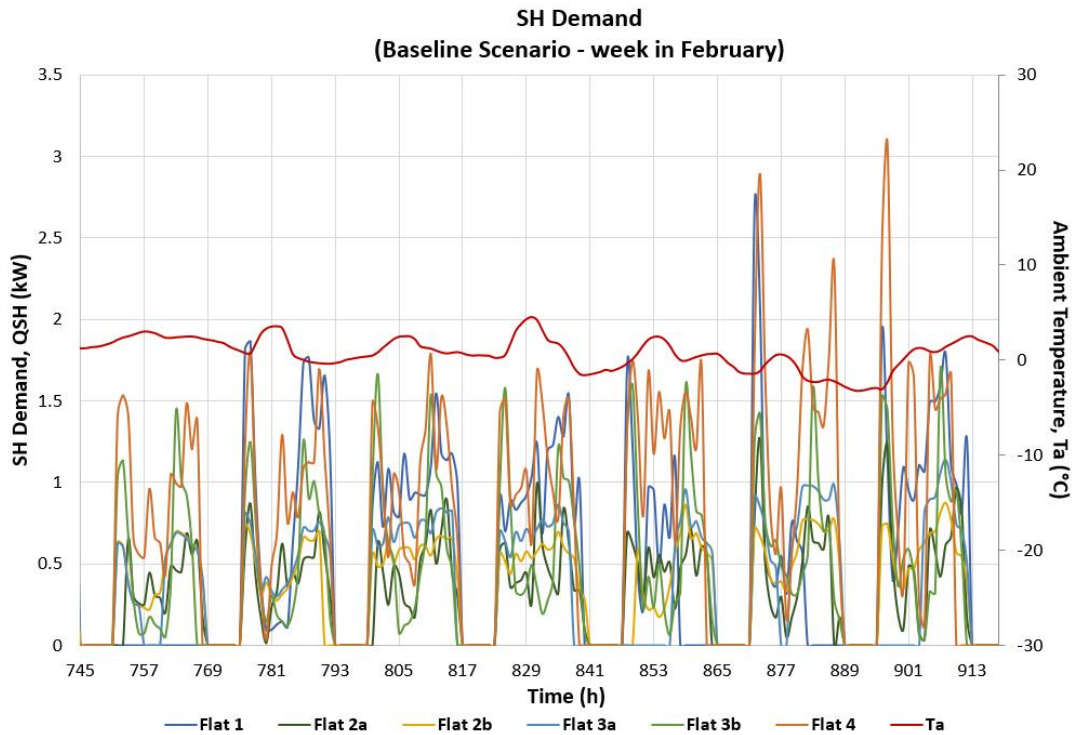


Figure 21. SH Demand of each flat (February week).

The hourly DHW profiles were generated using the DHWCalc tool. A 07:00-23:00 occupancy was assumed, and the SH profiles were modified based on this assumption and on the occupancy and activity assumptions made during the DHW profiles' generation.

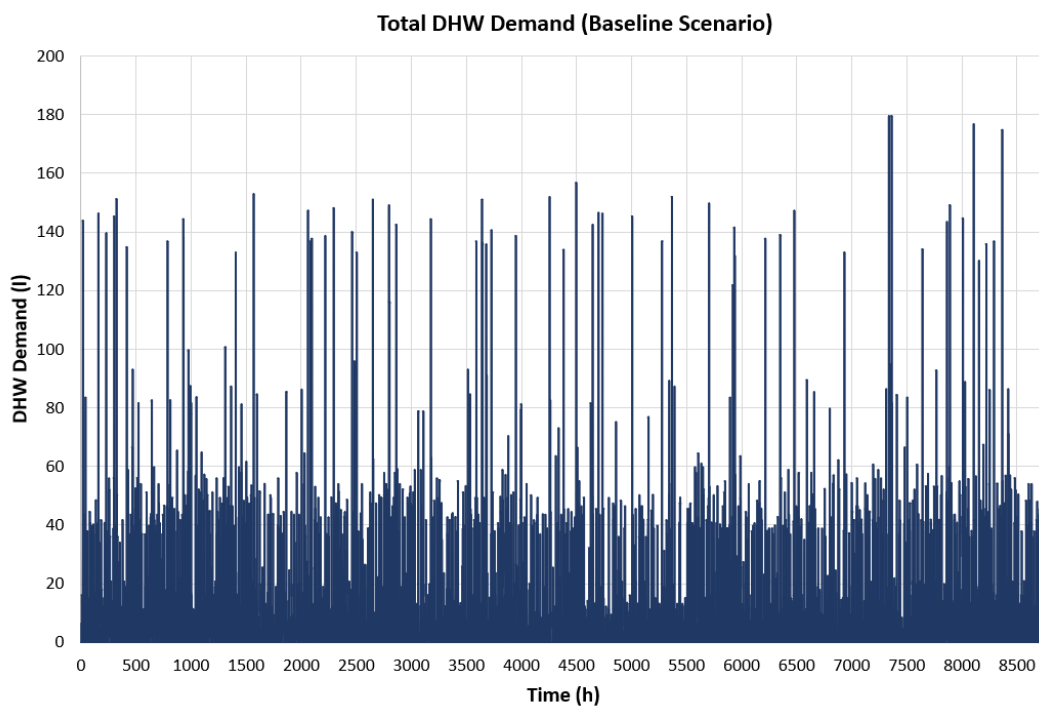


Figure 22. Baseline Scenario total DHW demand

Both profile types were scaled according to 2018 data from heat meters at the existing DH system and connected buildings, which were kindly shared with the Energy Systems Research Unit. The tank size for this scenario was set at 500l.

In the baseline system, there is one DH Substation per building. This means that Flats 2a and 2b –which are located in the same building- share a DH substation (SS), as do flats 3a and 3b. Consequently, since calculations for heating losses were done for the pipes connecting the EC to each SS, the two loads of each shared building were aggregated into one when calculating the DF of the network.

6.2. Scenario 1: Individual systems for neighbouring clusters of buildings

For this scenario, a second group of buildings, Cluster 2, was considered, located in the vicinity of Cluster 1. Assuming that the buildings of that cluster have similar properties and sizes to those investigated in the Baseline Scenario, the same profiles were used as a base for estimating their SH and DHW demand, after making slight modifications and using various scaling factors. The resulting demands were higher than those of Cluster 1 -especially the DHW demand- but follow similar patterns of use. The profiles are presented in **Fig** and, below. The same network topology assumptions as those of the Baseline Scenario were used for the Cluster 2.

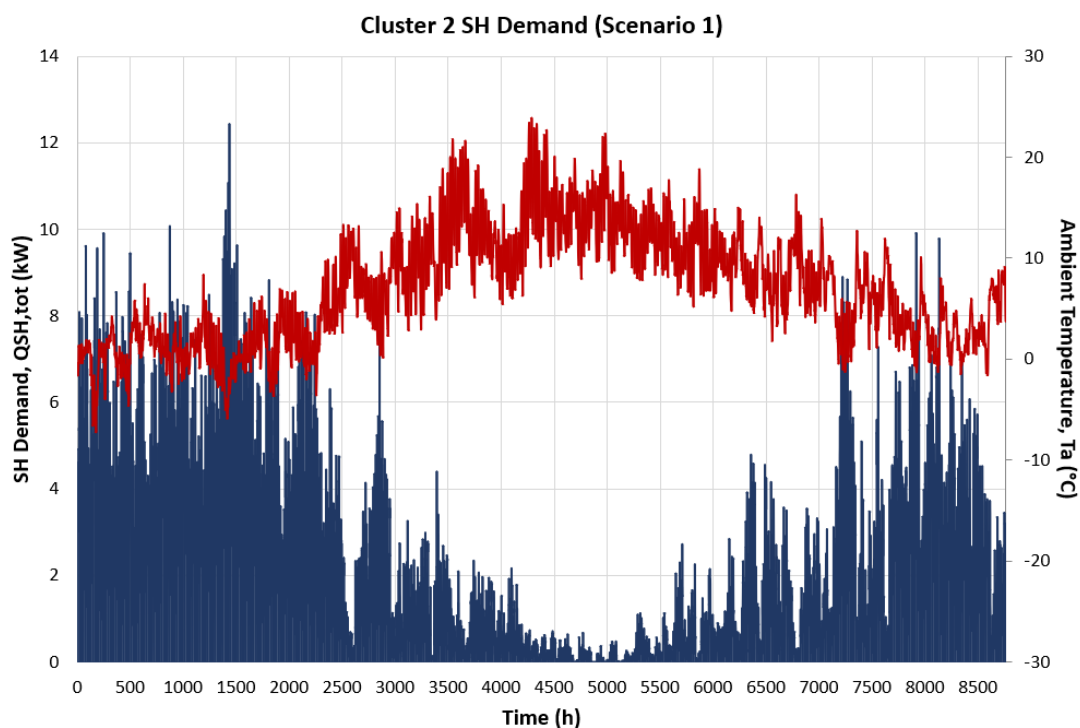


Figure 23. Scenario 1 total SH demand.

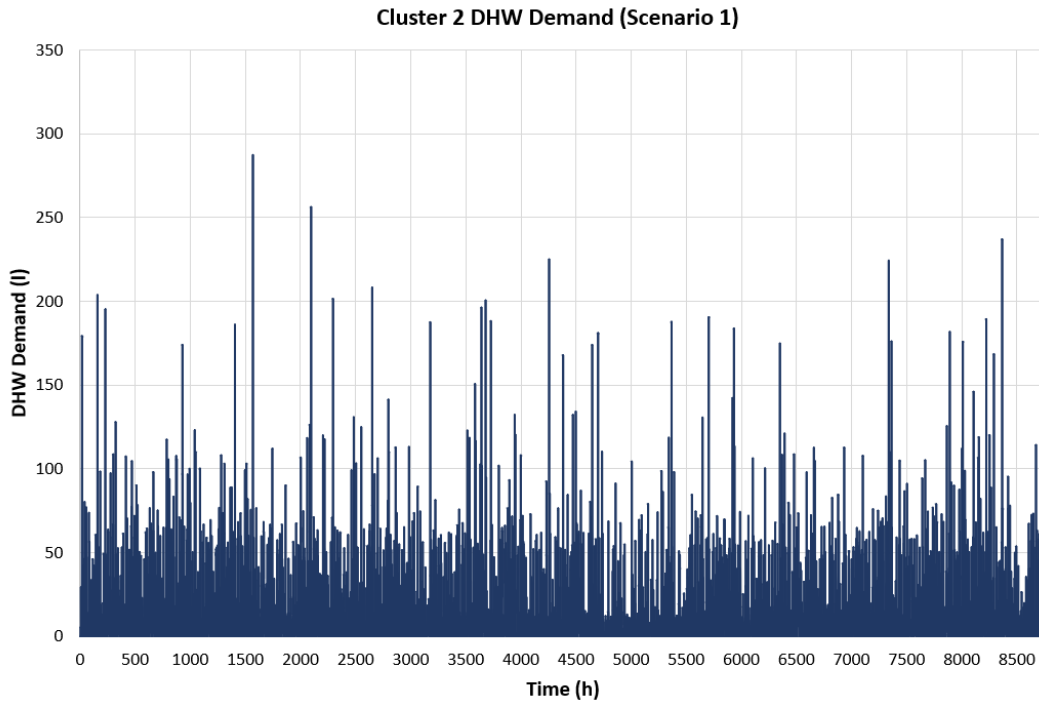


Figure 24. Scenario 1 total DHW demand

6.3. Scenario 2: Shared system for neighbouring clusters of buildings

In this scenario, it was assumed that both clusters of buildings are supplied by the same EC and network.

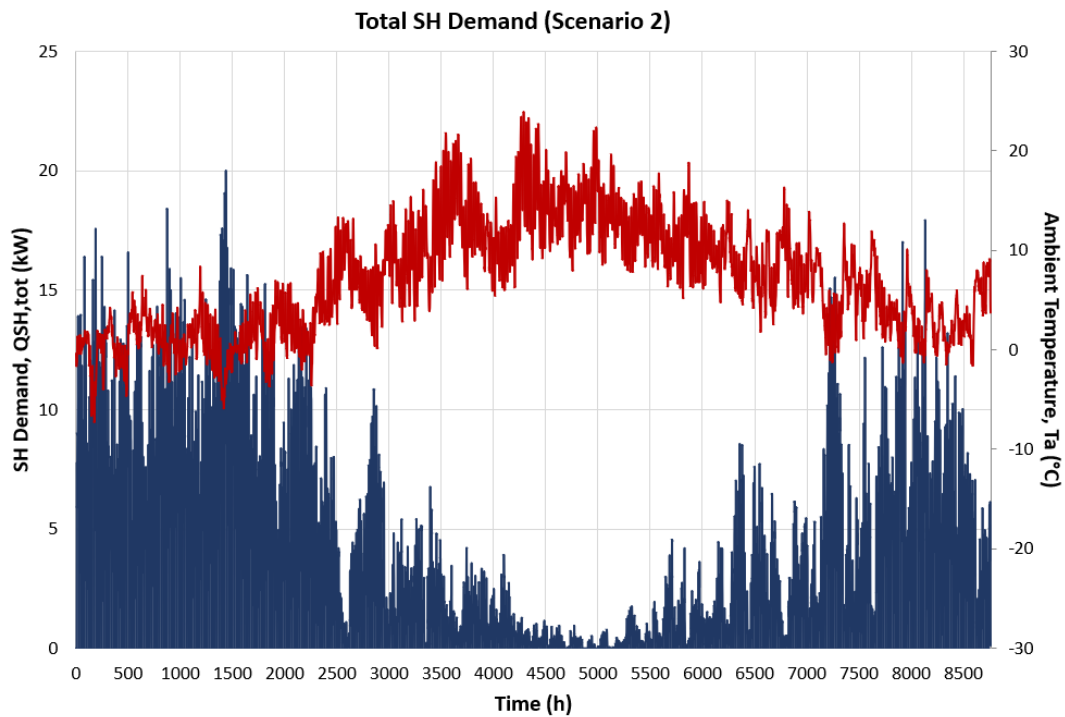


Figure 25. . Scenario 2 total SH demand.

Since the total SH demand is much higher than in the previous ones, a ASHP of larger capacity – split type Mitsubishi Ecodan PUHZ-SW200YKA-BS– was chosen and its performance data entered as parameters in the “Heat Pump” function. The charging flow for the heat pump was set at 300kg/h, since the resulting DHW demand (Fig) was higher much higher than that of the individual clusters. The overall heat losses of the network were estimated at around 15%.

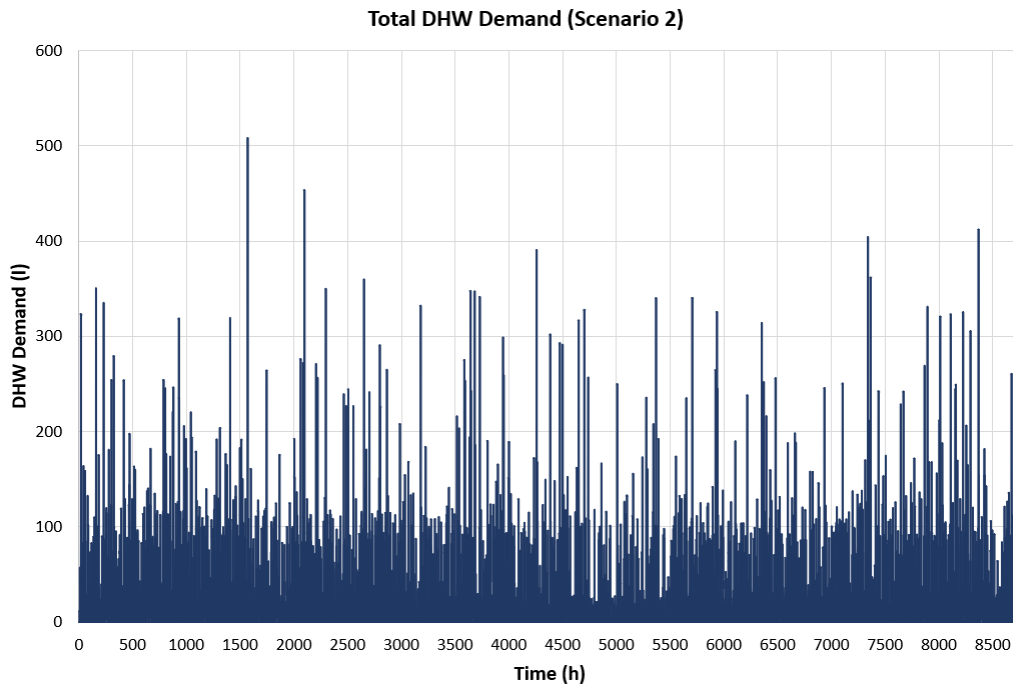


Figure 26. Scenario 2 total DHW demand

7. Results & Discussion

In the Baseline Scenario, the behaviour of the WST during a typical week in winter (first week of February), with high DHW demand, and a typical summer week (first week of July) with lower DHW demand and high solar energy generation, are presented in Fig. 27 and 28, as representative examples of how the WST model behaves under different conditions. The behaviour of the tank for Scenario 1 was very similar, which is why it is not included here.

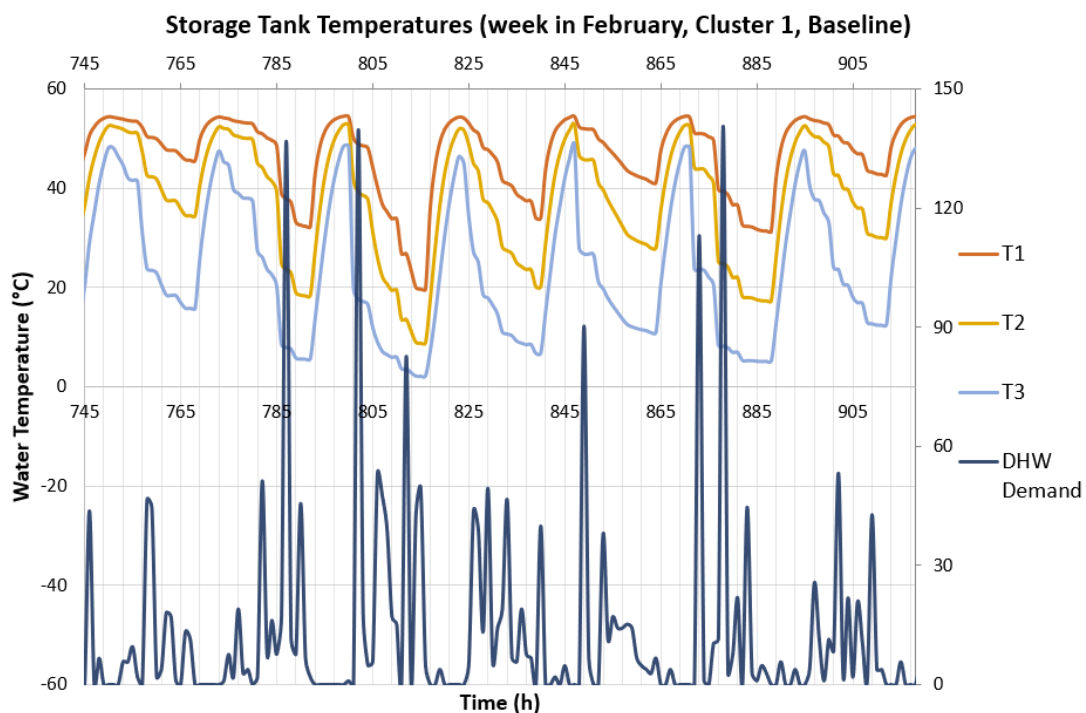


Figure 27. Baseline Scenario storage tank (February week).

In both figures, the temperatures of each node of the tank rise overnight, while the tank is charged by the ASHP, and drop during the day. Those temperature drops are particularly sharp in the case of the bottom node, $j = 3$, which receives an equal flow of cold water to the one that is drawn off from the consumers. In Fig it is also observed that in consecutive hours with relatively high demand, the tank is not able to supply DHW temperature above 50°C. This could be a result of the “charging” flow rate of the WST through the ASHP being fixed at 100 kg/h, of the absence of an auxiliary electric heater inside the WST in this model, and even of the size of the tank, which –under this charging strategy and time-step approach- cannot sufficiently heat and store the amount of water needed during such days.

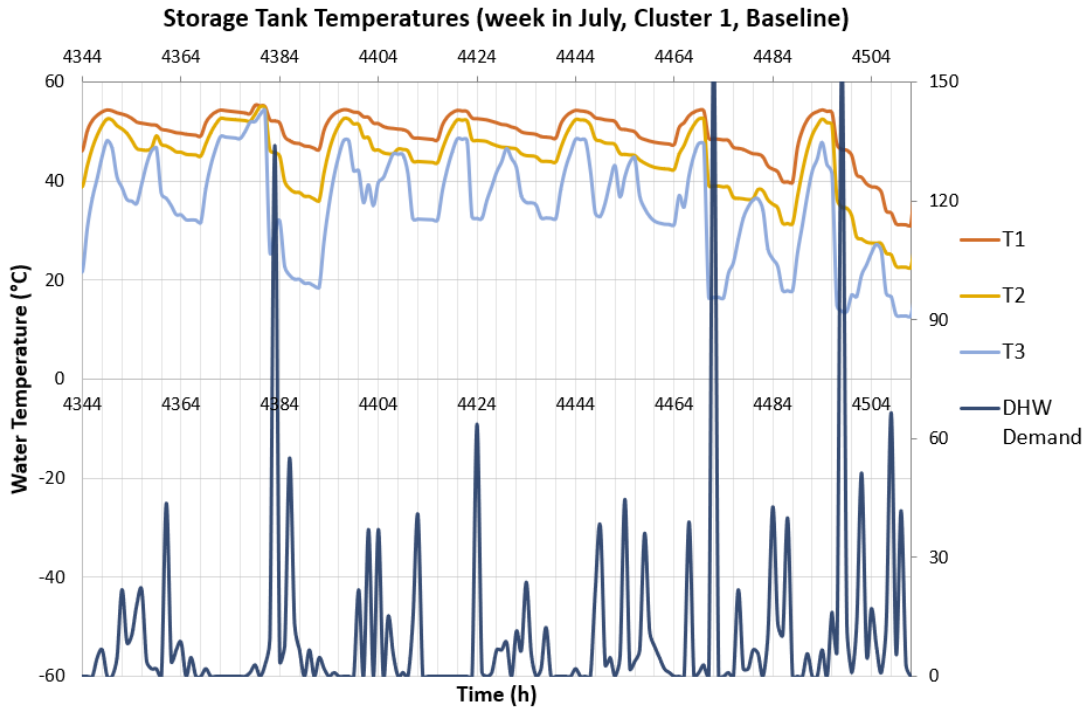


Figure 28. Baseline Scenario storage tank (July week).

The same sharp drops are also observed during the representative summer week, in Fig. 28. In this case it is also obvious how the tank copes quite well with hourly demands lower than 60 l, but not with the twice as large peaks that occur three times during this specific week.

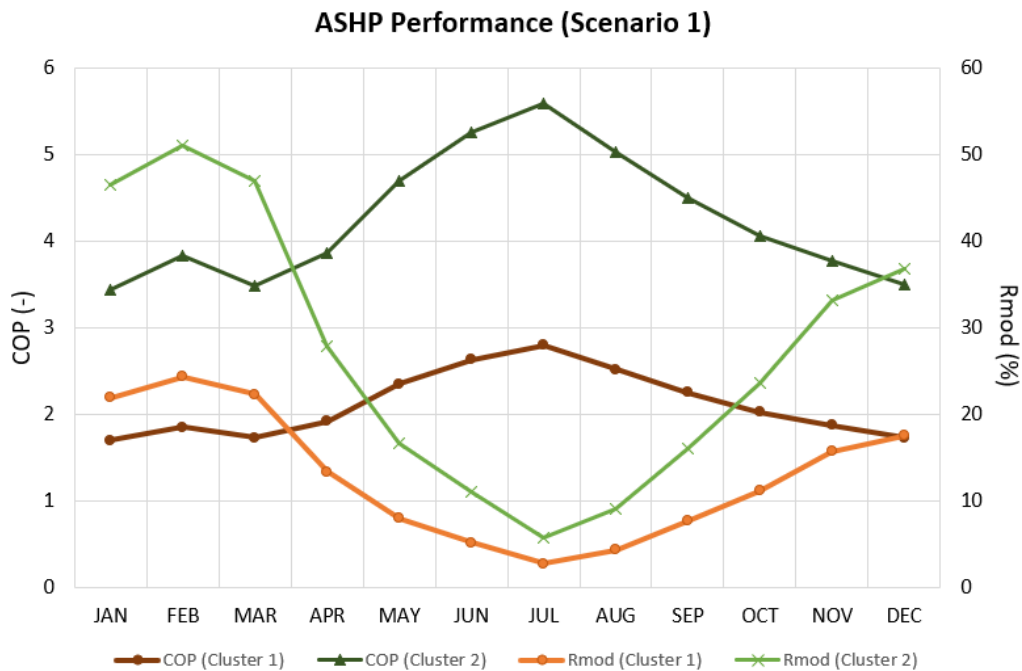


Figure 29. Performance comparison between the ASHPs of the individual DH schemes (Scenario 1).

The performance of the individual ASHPs for Clusters 1 and 2 are presented in Fig.29 , through the calculated average monthly COP and modulation level (Rmod) values. It is obvious that the ASHP capacity was too large for the buildings of Cluster 1, as the system was operating at a level well below 30% of the maximum thermal output of the ASHP throughout the year. In Scenario 1, since both groups of buildings had similar demand characteristics and their heating schemes were based on identical systems and operational principles, the yearly cost of electricity was almost exactly the same for both schemes.

In Scenario 2, where all buildings share the same DH system, the COP achieved by the chosen ASHP is not as high as the one achieved in the Baseline Scenario, since the maximum capacity is too large. However, the COP still reaches values over 3.0 in the summer months.

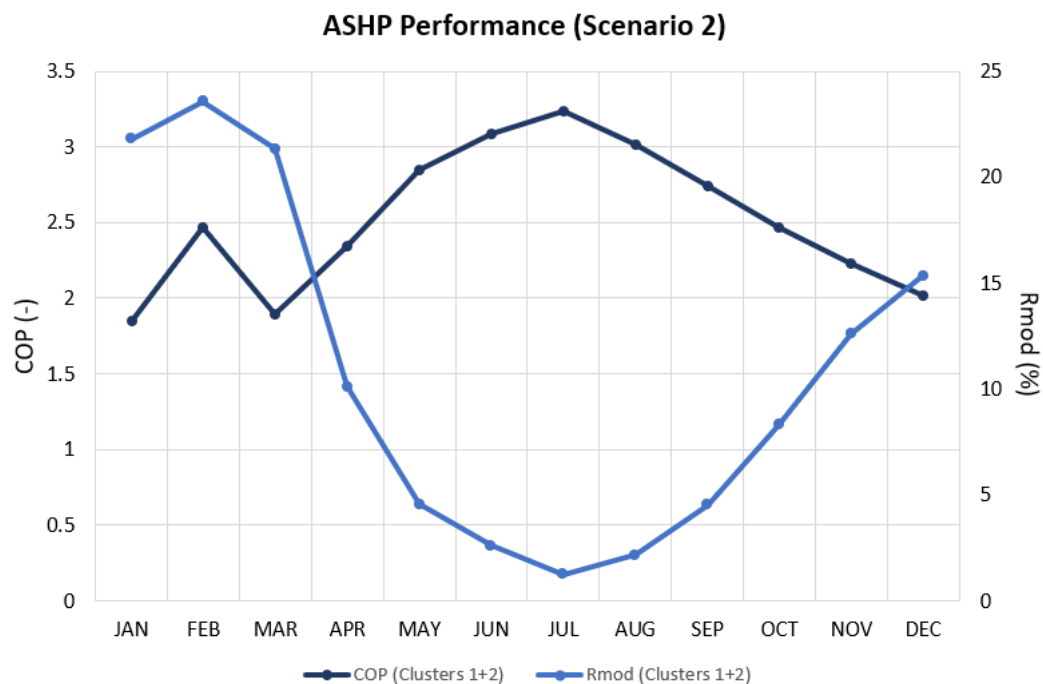


Figure 30. Performance of the shared ASHP (22kW) (Scenario 2).

8. Conclusions & Future Work

The model operates with given temperature, demand, and CO₂/cost profiles for the entire year, which implies that the calculations are based on historical data or perfect forecast.

The DHW consumption as metered for the case study is rather low compared with reference values for two-person households. This can be attributed to the fact that there could be only one occupant/flat or the occupants are inclined to use less water due to their lifestyles and/or environmental conscience. In any case, as indicated in relevant studies, DHW per dwelling can vary significantly even for dwellings of the same size, so it has to be seriously taken into account when designing systems that supply only a small number of consumers.

The proposed way of modelling the performance of the ASHP as a function of T_a and $T_{hp,out}$ provides a fast and straightforward way of expressing the Q_{th} and COP of each modulation level as a surface, thus quickly calculating the specific values for each given pair of $(T_a, T_{hp,out})$. However, it is clear that the fit is only based on a relatively small number of datapoints ($n=23$) and is not as satisfactory for all $T_{hp,o}$ values and modulation levels presented in this study. Additionally, the effect of the return water temperature from the network and/or the bottom node of the storage tank, which enters the condenser, has not been considered in the model. A different approach for higher output temperatures and the consideration of measured data for the performance of the given heat pump under various temperature differences along the condenser would surely yield a more precise model.

The model developed in this study was set up assuming that the ASHP can only supply either the SH circuit or the ST charging circuit during a time step, and never both of them simultaneously. Consequently, the ASHP could not be set to operate at a higher capacity level, which would allow it to perform both functions, at hours during day time when the grid CO₂ intensity dropped. This could be considered as a lost opportunity for charging the tank with “cleaner” energy. However, considering the time limitations of the project and the need to keep the resulting model as simple as possible, this was a

necessary simplification that allowed the modelling part of the project to be completed on time. Still, this is a case that is definitely worth investigating in future work.

The next step would be to integrate the topology and characteristics of the DH network into the model. This could be done by including the lengths of the main pipes and their heat loss coefficients (per unit pipe length) as parameters, and by adding a few equations that would calculate heat losses according to the method presented in Chapter 4.

The main limitation of this study was the complexity of the interconnections between the individual systems that comprise the investigated DH scheme -and any such scheme, for that matter- especially in terms of mass and heat transfer between two systems. Although a great effort was made in order to include those connections as accurately as possible in the model, the hourly time step that was employed, some rough assumptions, and the inevitable time constraints of this individual project did not allow this effort to be fully successful, especially in the case of the solar FPC modelling. Still, A more detailed cost analysis should also have been performed. It should have taken into consideration that additional costs occur in heating schemes based on renewable energy systems, due to the fact that auxiliary, fuel-powered energy systems are also included on the supply side (e.g. gas boilers or wood pellet boilers). This is common practice in order to ensure security of supply.

In this project, only the CO₂ emissions of the electricity used to power the ASHP were taken into consideration, since only the thermal side and temperature regimes of the simulated energy schemes were investigated. It would be useful, however, to also consider the hydraulics' side of the problem and the pumping work required to distribute hot water in every scenario. Pumps consume a fair amount of electricity as the volumetric water flows rise, so their contribution to CO₂ emissions should be monitored, as the simulated networks grow in size. When it comes to applying this methodology for comparison of different individual systems, with different manufacturing procedures, perhaps the total life cycle emissions of each system should also enter the equation.

References

- AES Solar, n.d. *Full Technical Specifications - AES Supremacy*, s.l.: s.n.
- Allison, J. et al., 2018. Assessing domestic heat storage requirements for energy flexibility over varying timescales. *Applied Thermal Engineering*, 25 5, Volume 136, pp. 602-616.
- Angrisani, G., Canelli, M., Roselli, C. & Sasso, M., 2014. Calibration and validation of a thermal energy storage model: Influence on simulation results. *Applied Thermal Engineering*, 67(1-2), pp. 190-200.
- Anon., 2009. *Tyfocor® Technical Information® = Registered Trademark Antifreeze Concentrate for protecting heating and cooling circuits from frost and corrosion Medium for heat pump systems Heat-transfer fluid-free of nitrites*, s.l.: s.n.
- Anon., 2014. *Degree days for energy management: A practical introduction*, s.l.: s.n.
- Anon., 2014. *RAUVITHERM AND RAUTHERMEX PRE-INSULATED PIPE*, s.l.: s.n.
- Anon., 2015. *ecodan Renewable Heating Technology DATA BOOK*. s.l.:Mitsubishi Electric Corporation.
- Anon., 2018. *Clean Growth - Transforming Heating - Overview of Current Evidence*, s.l.: s.n.
- Anon., 2018. *Clean Growth - Transforming Heating - Overview of Current Evidence December 2018*, s.l.: s.n.
- Anon., n.d. 00475681.
- Anon., n.d. *Accumulators Type Stratification Tank Series Multi-Fuel*, s.l.: s.n.
- Anon., n.d. building solutions for low temperature heat supply.
- Anon., n.d. *HYDRAULIC PIPING STANDARD HANDBOOK*, s.l.: s.n.
- Anon., n.d. pub-149-large-diameter-copper-tubes-pdf.
- Baetens, R. & Saelens, D., 2016. Modelling uncertainty in district energy simulations by stochastic residential occupant behaviour. *Journal of Building Performance Simulation*, 3 7, 9(4), pp. 431-447.
- Bee, E., Prada, A., Baggio, P. & Psimopoulos, E., 2019. Air-source heat pump and photovoltaic systems for residential heating and cooling: Potential of self-consumption in different European climates. *Building Simulation*, 1 6, 12(3), pp. 453-463.
- BizEE Weather Data for Energy Professionals, n.d. *Heating and Cooling Degree Days - Free Worldwide Data Calculation*. [Online]
Available at: <https://www.degreedays.net/>
- BRE Housing Centre, 2005. *Estimates of hot water consumption from the 1998 EFUS. Implications for the modelling of fuel poverty in England.*, s.l.: s.n.
- BSI Standards, 2017. *Energy performance of buildings - Method for calculation of the design heat load, Part 1: Space heating load, Module M3-3*. s.l.:s.n.

BSI Standards, 2017. *Energy performance of buildings - Method for calculation of the design heat load, Part 2: Explanation and justification of EN 12831-1, Module M3-3*. s.l.:BSI Standards Publication.

Carpaneto, E., Lazzeroni, P. & Repetto, M., 2015. Optimal integration of solar energy in a district heating network. *Renewable Energy*, Volume 75, pp. 714-721.

Chauvaud De Rochefort, H., 2018. *Market Report: Heat Networks in the UK*, s.l.: s.n.

Cheshire, D., Menezes, A. C. & Chartered Institution of Building Services Engineers., n.d. *Evaluating operational energy performance of buildings at the design stage*. s.l.:s.n.

Climate-Data.org, n.d. *Finhorn Climate: Average Temperature, weather by month, Finhorn weather averages - Climate-Data.org*. [Online]

Available at: <https://en.climate-data.org/europe/united-kingdom/scotland/findhorn-703458/>

Day, T., 2006. *Degree-days: theory and application - TM41: 2006*. London: The Chartered Institution of Building Services Engineers (CIBSE).

De Coninck, R. et al., 2014. Rule-based demand-side management of domestic hot water production with heat pumps in zero energy neighbourhoods. *Journal of Building Performance Simulation*, 7, 7(4), pp. 271-288.

Dinçer, I. & Rosen, M. (. A., 2011. *Thermal Energy Storage: systems and applications*. s.l.:Wiley.

Duffie, J. A. & Beckman, W. A., 2013. *Solar Engineering of Thermal Processes*. 4th Edition ed. s.l.:Wiley.

Ecovillage Findhorn, n.d. *Ecovillage Findhorn*. [Online]

Available at: <https://www.ecovillagefindhorn.com/>

Energy Monitoring Company & Energy Saving Trust, 2008. *Measurement of Domestic Hot Water Consumption in Dwellings*, s.l.: s.n.

European Commission, 2018. Improving energy and resource efficiency - Analytical Report. In: s.l.:s.n.

Hsieh, S., Omu, A. & Orehounig, K., 2017. Comparison of solar thermal systems with storage: From building to neighbourhood scale. *Energy and Buildings*, 110, Volume 152, pp. 359-372.

IEA, 2018. *Statistics European Union 28 - Heat generation by fuel*. [Online]

Available at:

<https://www.iea.org/statistics/?country=EU28&year=2016&category=Heat&indicator=HeatGenByFuel&mode=chart&dataTable=ELECTRICITYANDHEAT>

Jordan, U. & Vajen, K., 2001. Influence Of The DHW Load Profile On The Fractional Energy Savings: A Case Study of a Solar Combi-System with TRNSYS Simulations. *Solar Energy*, 7, Volume 69, pp. 197-208.

Jordan, U., Vajen, K. & Braas, H., 2017. *Manual DHWcalc: Tool for the Generation of Domestic Hot Water (DHW) Profiles on a Statistical Basis - Version 2.02b (March 2017)*. s.l.:Universität Kassel Institut für Thermische Energietechnik Solar und Anlagentechnik.

- Kalaiselvam, b. S., Parameshwaran, R., York, N. & Diego, S., 2014. *Thermal Energy Storage Technologies for Sustainability Systems Design, Assessment and Applications*, s.l.: s.n.
- Kalogirou, S. A., 2014. *Solar Energy Engineering: Processes and Systems*. 2nd Edition ed. s.l.:Academic Press.
- Kelly, N. J. & Cockroft, J., 2011. Analysis of retrofit air source heat pump performance: Results from detailed simulations and comparison to field trial data. *Energy and Buildings*, 1, 43(1), pp. 239-245.
- Klein, B., 2012. Independent testing of heat pumps is needed for reliable COP. *The REHVA European HVAC Journal*, 10, 49(5), pp. 15-18.
- Kleinbach, E. M., 1990. *Performance Study of One-Dimensional Models for Stratified Thermal Storage Tank*, MSc Thesis, s.l.: s.n.
- Koiv, T.-A., Mikola, A. & Toode, A., 2013. DHW Design Flow Rates and Consumption Profiles in Educational, Office Buildings and Shopping Centres. *Smart Grid and Renewable Energy*, 16 10, 04(03), pp. 287-296.
- Larsen, H. V., Bøhm, B. & Wigbels, M., 2004. A comparison of aggregated models for simulation and operational optimisation of district heating networks. *Energy Conversion and Management*, 5, 45(7-8), pp. 1119-1139.
- Li, H. ;. et al., n.d. *Future low temperature district heating design guidebook Final Report of IEA DHC Annex TS1. Low Temperature District Heating for Future Energy Systems*, s.l.: s.n.
- Li, H. ;. et al., n.d. *General rights Future low temperature district heating design guidebook Final Report of IEA DHC Annex TS1. Low Temperature District Heating for Future Energy Systems*, s.l.: s.n.
- Lund, H. et al., 2018. *The status of 4th generation district heating: Research and results*. s.l.:Elsevier Ltd.
- Maclean, K., Sansom, R., Watson, T. & Gross, R., 2016. *Managing Heat System Decarbonisation Comparing the impacts and costs of transitions in heat infrastructure Final Report Acknowledgment*, s.l.: s.n.
- Mahooti, M., 2017. *NREL's Solar Position Algorithm - File Exchange - MATLAB Central*. [Online]
Available at: <https://uk.mathworks.com/matlabcentral/fileexchange/59903-nrel-s-solar-position-algorithm-spa>
- Manfren, M., Caputo, P. & Costa, G., 2011. *Paradigm shift in urban energy systems through distributed generation: Methods and models*. s.l.:Elsevier Ltd.
- National Grid, 2017. Carbon Intensity Forecast Methodology. 12.
- National Grid, Environmental Defense Fund Europe, University of Oxford & WWF, n.d. *Carbon Intensity API*. [Online]
Available at: <https://carbonintensity.org.uk/>
- Newton, B. J., 1995. *Modeling of Solar Storage Tanks*, MSc Thesis, s.l.: s.n.

- Østergaard, P. A. & Andersen, A. N., 2016. Booster heat pumps and central heat pumps in district heating. *Applied Energy*, 15 12, Volume 184, pp. 1374-1388.
- Pálsson, H. et al., 1999. *Equivalent models of district heating systems for on-line minimization of operational costs of the complete district heating system*. s.l.:Department of Energy Engineering, Technical University of Denmark.
- Panaras, G., Mathioulakis, E. & Belessiotis, V., 2013. Investigation of the performance of a combined solar thermal heat pump hot water system. *Solar Energy*, 7, Volume 93, pp. 169-182.
- Pfenninger, S. & Staffell, I., 2016. Long-term patterns of European PV output using 30 years of validated hourly reanalysis and satellite data. *Energy*, 1 11, Volume 114, pp. 1251-1265.
- Quaschnig, V., 2016. *Understanding Renewable Energy Systems*. 2nd Edition ed. s.l.:Routledge.
- REHAU, 2013. *Rauvitherm and Rauthermex Pre-Insulated Pipe*. [Online] Available at: <https://www.rehau.com/download/1347030/pre-insulated-technical-manual.pdf>. [Accessed 2 7 2019].
- Rehman, H. u., Hirvonen, J. & Sirén, K., 2018. Performance comparison between optimized design of a centralized and semi-decentralized community size solar district heating system. *Applied Energy*, 1 11, Volume 229, pp. 1072-1094.
- Reinholdt, L. ; et al., 2019. Heat pump COP, part 1: Generalized method for screening of system integration potentials. *Citation*, Volume 2, pp. 1097-1104.
- SAV Systems, 2015. *Design and Product Guide: Danfoss FlatStations*, s.l.: s.n.
- Schmidt, D., 2018. *Low Temperature District Heating for Future Energy Systems*. s.l., Elsevier Ltd, pp. 595-604.
- Scottish Government, 2015. *Energy in Scotland 2015*, s.l.: s.n.
- Stanciu, C., Stanciu, D., Gheorghian, A. & Şoriga, I., 2016. *Analysis of a flat plate collector for hot water domestic use - A sensitivity study*. s.l., Institute of Physics Publishing.
- Stark, S., Loose, A. & Drück, H., 2014. *Field test results from combined solar thermal and air-source heat pump systems with a special focus on defrosting*. s.l., Elsevier Ltd, pp. 654-663.
- Thevenard, D. & Haddad, K., n.d. *Development of a Stratified Tank Model with Immersed Heat Exchangers in ESP-r*, s.l.: s.n.
- van der Heijde, B., Aertgeerts, A. & Helsen, L., 2017. Modelling steady-state thermal behaviour of double thermal network pipes. *International Journal of Thermal Sciences*, 1 7, Volume 117, pp. 316-327.
- Vandermeulen, A., van der Heijde, B. & Helsen, L., 2018. *Controlling district heating and cooling networks to unlock flexibility: A review*. s.l.:Elsevier Ltd.
- Wallentén, P., 1991. *Steady-state heat loss from insulated pipes*, *Licentiate*, s.l.: Byggnadsfysik LTH, Lunds Tekniska Högskola.

Watkins, D. E., 2011. *Heating Services in Buildings - Design, Installation, Commissioning and Maintenance*. s.l.:John Wiley & Sons.

Werner, S., 2017. *International review of district heating and cooling*. s.l.:Elsevier Ltd.

Wiltshire, R., Williams, J. & Woods, P., n.d. *A technical guide to district heating*, s.l.: s.n.

Woods, P., Chartered Institution of Building Services Engineers., AECOM (Firm) & Association for Decentralised Energy., 2015. *Heat networks : code of practice for the UK : raising standards for heat supply*. s.l.:CIBSE, Chartered Institute of Building Services Engineers.

Zelzouli, K., Guizani, A., Sebai, R. & Kerkeni, C., 2012. Solar Thermal Systems Performances versus Flat Plate Solar Collectors Connected in Series. *Engineering*, 04(12), pp. 881-893.

Zelzouli, K., Guizani, A., Sebai, R. & Kerkeni, C., 2012. Solar Thermal Systems Performances versus Flat Plate Solar Collectors Connected in Series. *Engineering*, Volume 4, pp. 881-893.

APPENDIX A: MATLAB Model

Main Matlab Programme

```

% Small-scale District Energy Systems Comparison Tool

% Parameters (set values in the script):
steps = 8761; %for hourly data
dt = 1; %time step = 1 h
tank_steps = 4; %dt=15min - 4 steps for each hour
Ntank = 3; % 3 nodes in the stratified tank
Nsolar = 2; % 2 solar arrays (of N panels each)
cp_w = 4.180; %kJ/(kg*K)
Qthmax = 14.000; % max HP capacity (kW)
% Distribution loss factor (first estimation)
LF = 0.150; % 10% of the SH & DHW heat leaving the plant will
be lost

% Assumption for HP control strategy:
%     mhp,tot/dt=fixed (for any t), Thp,i=variable
% Max allowed mass flow initialisation (max values):
mSHp_max = 0; %will be calculated based on the max load from
the SHprofile
mhpt_max = 500.000; %kg/h, max for the copper pipe DN25 = 1080
mhptot_max = 0; %will be calculated after mSHp_max

% Variable values for the entire simulation time:
HourlymSHp = zeros(steps,1); % total mass flow that covers SH
demand
Hourlymhpt = zeros(steps,1); % mass flow in the HP-tank
charging loop
HourlyRmod = zeros(steps,1); % modulation ratio of the HP
HourlyPerfHP = zeros(steps,4); % [Tshp,o, Qsh,tot, Qt,charge,
COP]
HourlyTempSolar = zeros(steps,2); % could turn to size=4 if I
consider losses!
HourlyOutputSolar = zeros(steps,2); % [Qsu,ηsu]
HourlyTempTank = zeros(steps,7); % Storage input & output
temps
HourlyCapTank = zeros(steps,1); % Storage content (kJ)
HourlyTankMode = zeros(steps,4); % logical variable:
% (t,1)=1 : the tank is charged by
the HP
% (t,2)=1 : the tank is charged by
the ST
% (t,3)=1 : the tank is charged by
the DHI
% (t,4)=1 : the tank is being
discharged
% (t,:)=0 : the tank is idle (only
losses)
% will be charged during the 1st
time step!
HourlyQch = zeros(steps,1); % Qcharge, energy input from the
HP to the tank
HourlyQel = zeros(steps,1); % Qel, energy input from
el.resistance to the tank

% Set/Target temperatures of water leaving the plant:

```

```

HourlyPerfHP(:,1) = 55.000; %Tshp,o=55C, same for the entire
year (?)
HourlyTempTank(:,2) = 55.000; %Tdhwp,o=55C, same for the
entire year (?)
%HourlyTempSolar(1,1) = 16.000; %Tsi=16C
% (min?) Supply & return temps @ consumers
TSHc_i = zeros(steps,1); TSHc_o = zeros(steps,1); TDWc_i=
zeros(steps,1);
TDHwc_i = zeros(steps,1);
TSHc_i(:,1) = 50.000; TSHc_o(:,1) = 25.000; TDHwc_i(:,1) =
50.000;
DTSHc = zeros(steps,1); DTSHc(:,1) = TSHc_i(:,1) -
TSHc_o(:,1);
% Temperature setpoint:
TmidSet = 52.000; % the HP charging is activated for this
node2 temp
DTsolAct = 5; % the ST is activated for this DT=Tsol,o-T2

%CapTankset = 10.000; % the kWh I want as stored water...be an
average...
                                %maybe predicted/forecasted?? to last a
few days??

% Dummy variables
Qth = zeros(steps,1); %Qth stored here before passed to the HP
function
mhptot = zeros(steps,1);

%Read data from weather file
DataWeather = xlsread('ambient_data.xlsx');
%Read data from water mains file
TempMains = xlsread('watermains_data.xlsx');
%Read energy centre internal temperature from file
TempEC = xlsread('storagetemp_data.xlsx');

%Read data from incidence angle modifier file (for  $\beta=57$ deg)
Ktheta = xlsread('Ktheta.xlsx');

%Read data from demand files (last column of the file = total
demand)
DataSHDemand = xlsread('SHdemand_data_cluster2.xlsx'); %Qsh,
kW/h
DataDHWDemand = xlsread('DHWdemand_data_cluster2.xlsx');
%Qdhw, L/h
%Read data from grid file
%DataGrid = xlsread('grid_data.xlsx');
%Read data from overnight schedule file:
DataNight = xlsread('night_schedule.xlsx');
Night = DataNight(:,2); % 2nd column contains the
nightschedule
                                % 1: night hour available for charging
(low tariff)

%Needed to calculate temp inside the energy centre for the
entire year
HourlyTempTank(:,7) = TempEC;

```

```

%Initialise tank node temps
TempTankNodes = zeros(1,Ntank); CapTankNodes = zeros(1,Ntank);
TinTank = zeros(1,7);
TempTankNodes(:) = [55 42 28] ; %initial temperatures of the
nodes (for t=0)
HourlyTempTank(:,1) = TempMains;
HourlyTempTank(1,5) = TempTankNodes(2); %HourlyTempTank(1,:) =
[0 30 0 0 27 0];
CapTankLevel = 0;
TempSolar = zeros(1,2);

%Calculate max SH main supply pipe flow rare based on max load
from data
mSHp_max = max(DataSHDemand(:,end))/...
           (cp_w*DTSHc(1))*3600; % kg/h

for t=1:dt:steps; % should it begin from 1? YES --it won't
enter the wrong loops
    % there could be DHW demand --regardless of charging or
not
    FlowTank(1) = DataDHWDemand(t,end);
    if (FlowTank(1)>0); HourlyTankMode(t,4)=1; end %there is
DHW discharge
    FlowTank(2:3) = 0;%no Qinputs

    %check the previous tank temps(t-dt) at every new step(t):
    if (Night(t)==1); % 00:00-07:00 period
        % assumption: no SH demand, only charging (if needed)
        if
            ((TempTankNodes(2)==TmidSet) || (TempTankNodes(2)<TmidSet));%nee
ds charging
                HourlyTankMode(t,1) = 1; %charging from the HP
                Hourlymhpt(t) = 300; %L/h
                HourlyQch(t) = Hourlymhpt(t)*cp_w/3600*...
                    (HourlyPerfHP(t,1)-TempTankNodes(2)); %Qch
from this mhpt & temps (kW)
                Win(:) = DataWeather(t,2:end);
                PerfHP = HourlyPerfHP(t,:); %(Tshp,o is already
loaded!)
                %Calculate actual heat to be provided by the HP
(call HP function):
                Qth(t) = HourlyQch(t); PerfHP(3) = Qth(t);
                [PerfHP] = heatpump(Win, PerfHP);
                HourlyPerfHP(t,:) = PerfHP;
                %mhp needed for charge, based on the actual
Qth,hp:
                Hourlymhpt(t) = PerfHP(3)*3600/...
                    (cp_w*(HourlyPerfHP(t,1)-TempTankNodes(2)));
                %prepare the flow input (STORAGE function called
outside the loop)
                FlowTank(2) = Hourlymhpt(t); %input as kg/h
            end
        else % 07:00 - 23:00 period
            % assumption: the HP supplies SH only

```

```

Win(:) = DataWeather(t,2:end); %used by both HP &
SOLAR functions
    if (DataSHDemand(t,end)>0);
        %Calculate needed flow to cover current total SH
demand, mSH,p(t)
        Qth(t) = DataSHDemand(t,end)*(1.000 + LF);
        HourlymSHp(t) = Qth(t)*3600/(cp_w*DTSHc(t)); %
kg/h
        PerfHP = HourlyPerfHP(t,:); %(Tshp,o is already
loaded!)
        %Calculate actual heat to be provided by the HP
(call HP function):
        PerfHP(3) = Qth(t);
        [PerfHP] = heatpump(Win, PerfHP);
        HourlyPerfHP(t,:) = PerfHP;
        %mhp needed for SH demand, based on the actual
Qth,hp:
        HourlymSHp(t)= PerfHP(3)*3600/...
        (cp_w*(HourlyPerfHP(t,1)-TempTankNodes(2))); %
kg/h
    end
    %check if there will be solar heat generation:
    if (Win(2)>0); % sunshine check
        %initialise solar function arguments (Win already
initialized)
        %insert current values as inputs
        HourlyTempSolar(t,1) = TempTankNodes(3); % Ts,i(t)
= T3(t-dt)
        TempSolar = HourlyTempSolar(t,:);
        %call solar function
        Kth=Ktheta(t);
        [OutputSolar,TempSolar] = solar(Win, TempSolar,
Kth);
        if ((TempSolar(2)-TempTankNodes(2))>=DTsolAct);
            TempSolar(1) = TempTankNodes(3);
            [OutputSolar,TempSolar] = solar(Win,
TempSolar, Kth);
            %store Qsol,ηsol for this step
            HourlyOutputSolar(t,:) = OutputSolar;
            HourlyTempSolar(t,:) = TempSolar;
            HourlyTempTank(t,3) =
HourlyTempSolar(t,2);%Tsol,out=T3,in
            HourlyTankMode(t,2) = 1;
            % considering solar coil efficiency factor
e=0.7
            FlowTank(3) = 0.7*OutputSolar(1); %maybe also
consider losses?
        end
    end
end % "Night" check
if (t>1); %so that the temps are not lowered (losses)
during t=0
    TinTank = HourlyTempTank(t,:);
    [TempTankNodes, CapTankLevel] = ...
        storage(FlowTank, TinTank, TempTankNodes);

```

```
        HourlyTempTank(t,2) = TempTankNodes(1);
        HourlyTempTank(t,5) = TempTankNodes(2);
        HourlyTempTank(t,6) = TempTankNodes(3);
    end
    HourlyCapTank(t,:) = CapTankLevel;
end
filename = 'results_2nd_total.xlsb';
xlswrite(filename,HourlyPerfHP,1)
xlswrite(filename,Hourlymhpt,2)
xlswrite(filename,HourlyTankMode,3)
xlswrite(filename,HourlyTempTank,4)
xlswrite(filename,HourlyCapTank,5)
xlswrite(filename,HourlyTempSolar,6)
xlswrite(filename,HourlyOutputSolar,7)

% writetable(HourlyTempTank, 'TempTank.xlsx','Delimiter',';')
% writetable(HourlyTankMode, 'TankMode.xlsx','Delimiter',';')
% writetable(HourlyQch, r, 'Qch.xlsx','Delimiter',';')
% writetable(Hourlymhpt, r, 'mhpt.xlsx','Delimiter',';')
% writetable(HourlyPerfHP, r, 'PerfHP.xlsx','Delimiter',';')
% writetable(HourlyOutputSolar, r,
'OutputSolar.xlsx','Delimiter',';')
```

```

function [Solar, Temps] = solar(Weather, Temps, K)
% Flat plate collector properties
% Absorber Area (m^2):
Aabs = 2.310;
% Heat loss coefficients, a1 (W/(m^2*K)), a2 (W/(m^2*K^2))
a1 = 4.021; a2 = 0.022;
% Optical (zero loss) efficiency, η0:
n0 = 0.781;
% Working medium properties (water)
% Heat capacity of water-antifreeze mixture, cp (kJ/(kg*K)):
cp_s = 2.780;

% Number of collectors:
Ns = 3;
% Mass flow rate (kg/s):
ms = 0.02*Aabs;
% Incidence angle modifier, Kθ
% for single-glazed collector:
b0 = 0.100;
% Kθ = 1.000 - b0*(1.000/cosd(Theta) - 1.000); %theta in
deg!
% Kθ = 1.000;

DT=zeros(1,1);
% Reduced ΔT between the collector & the ambient air:
DT(1,1) = Temps(1) - Weather(1);
% DT(1,1) = (Temps(1) + Weather(1))/2;
% Useful energy output of the collector (W)
Solar(1) = Aabs*(n0*K*Weather(2) - a1*DT - a2*(DT^2));

if (Solar(1)<0);
    Solar = [0 0];
else
    % Efficiency of the collector
    Solar(2) = n0*K - a1*DT/Weather(2) - a2*(DT^2)/Weather(2);
    % Temperature of fluid at collector output
    Temps(2) = Temps(1) + Ns*Solar(1)/(ms*1000*cp_s);
end
end

function [Tj, Est] = storage(Inputs, Temps, Tj)
% function [Tj, Ej] = storage(Inputs, Temps, Tj)
% Solving a dT(t)/dt = A * T(t) + D DE system w/ the Crank-
Nicolson method
% Tj, Ej: contain node temps & energy contents of the previous
time step
% (init. values) & are updated by this function, then
passed to "main"

%input flows should be in kg/h

% Water tank properties
% Height (m):

```

```

Hst_o = 2.15;
% Diameter (m) (without insulation):
Dst_o = 1.15;
% U value (W/(m^2/K)):
Ust = 0.45;
% Insulation thickness (m):
dins = 0.100; %assumption: it's uniform everywhere
% % Insulation thermal conductivity (W/(m*K)):
% kins = 0.02;

% Internal Dimensions (m):
Hst_i = Hst_o - 2*dins; %assumption: insulation both at top &
bottom
Dst_i = Dst_o - 2*dins;
% Water volume (L):
Vst = 1000*pi*Hst_i*(Dst_i/2)^2; % *1000 to covert m^3 to L

% Water properties (assumed constant):
cp_w = 4.180; %kJ/kgK
rho_w = 1.000; %kg/L

% Node calculations:
N = 3;
% Height (m), volume (L), water mass (kg):
Hj = Hst_i/N; Vj = Vst/N; Mj = rho_w*Vj; % same for all nodes
% External surface area, Aj:
Aj = zeros(1,N);
Aj(1) = pi*Dst_i*(Hj + Dst_i/4); Aj(2) = pi*Dst_i*Hj; Aj(3) =
Aj(1);

% Initilisation:
alpha = [1 0 0]; % 1: there is an auxiliary water inlet in
node j
beta = [0 0 1]; % 1: there is a mains water inlet in node j
gamma = [0 0 0]; % values will later change
(=f(alpha,beta,flows))
delta = [0 0 1]; % 1: there is a solar heat exchanger in node
j
c_low = zeros(5,N); C_up = zeros(2,N); A = zeros(N,N); D =
zeros(1,N);
A=zeros(3,3);

% Reference Temperature = Bottom node temperature
Tref = Tj(3);

% Initilisation of temperatures & energy contents:
Tst_m = 0;
%Temps(7) = Temps(7) + 3; % Tec = Tamb + 3
Tnew = zeros(1,N); TnewX = zeros(1,N);
Eold = zeros(1,N); Enew = zeros(1,N);
Tnew = Tj; %Tj comes in loaded with the node temps of the prev
steps
% and leaves with the new temps

%calculate prev energy content (before charging, with prev Tj)
for j=1:1:N;

```

```

    Eold(j) = Mj*cp_w*(Tj(j) - Tref); % Ej=f(Tj-Tec) [kJ]
end

gamma(1) = -Inputs(1)*sum(beta(2:end));
gamma(2) = Inputs(2)*alpha(1) - Inputs(1)*beta(end);
gamma(3) = Inputs(2)*sum(alpha(1:2));

% Constants for each hour:
c_low(1,:) = alpha(:)*Inputs(2)/Mj; % 1/h
c_low(2,:) = beta(:)*Inputs(1)/Mj; % 1/h
c_low(3,:) = Ust*3600*Aj(:)/(Mj*cp_w*1000); % 1/h
%converting cp_w to J/kgK and Ust to J/h
c_low(4,:) = gamma(:)/Mj; % 1/h
c_low(5,:) = delta(:)*(Inputs(3)*3600)/(Mj*cp_w*1000); % 1/h
(Qsol in J/s)
%converting Qsol from J/s to kJ/h

% construct D matrix and dummy matrices (useful for matrix A):
for j=1:1:N;
    C_up(1,j) = -sum(c_low(1:4,j)); %for gamma(j)>0
    C_up(2,j) = -sum(c_low(1:3,j)) + c_low(4,j); %for
gamma(j)<0
    D(j) = c_low(1,j)*Temps(2) + c_low(2,1)*Temps(1) +
c_low(3,j)*Temps(7) + ...
    c_low(5,j);
end

%construct A matrix using the mixing vector:
if (gamma(1)>0);
    A(1,:) = [C_up(1,1);0;0];
else
    A(1,:) = [C_up(2,1);-c_low(4,1);0];
end
if (gamma(2)>0);
    A(2,:) = [c_low(4,2);C_up(1,2);0];
else
    A(2,:) = [0;C_up(2,2);-c_low(4,2)];
end
if (gamma(3)>0);
    A(3,:) = [0;c_low(4,3);C_up(1,3)];
else
    A(3,:) = [0;0;C_up(2,3)];
end

dt = 1; ie=0; err =2; dTs = zeros(1,3);
while (abs(err)>0.03);
    TnewX1=0;
    Told1 = Tnew(1); Told2 = Tnew(2); Told3 = Tnew(3);
    TnewX(1) = dt*(A(1,1)*(Tj(1)+Tnew(1))/2 +
A(1,2)*(Tj(2)+Tnew(2))/2 ...
    + D(1)) + Tj(1);
    TnewX(2) = dt*(A(2,1)*(Tj(1)+Tnew(1))/2 +
A(2,2)*(Tj(2)+Tnew(2))/2 ...
    + A(2,3)*(Tj(3)+Tnew(3))/2 + D(2)) + Tj(2);
    TnewX(3) = dt*[A(3,2)*(Tj(2)+Tnew(2))/2 +
A(3,3)*(Tj(3)+Tnew(3))/2 ...

```

```

        + D(3)] + Tj(3);
TnewX1 = sort(TnewX, 'descend');
Tnew = TnewX1;
ie = ie+1; %iteration counter
dT(1) = abs(Tnew(1)-Told1); dT(2) = abs(Tnew(2)-Told2);
dT(3) = abs(Tnew(3)-Told3);
err = max(dTs);
end
%calculate energy content for these temperatures
for j=1:1:N;
    Enew(j) = Eold(j) + Mj*cp_w*(Tnew(j) - Tj(j));
end
Tst_m = Vj*sum(Tj)/Vst; %new Tmean
Tref = Tnew(3);
Est = Vst*cp_w*(Tst_m-Tref);

Tj = Tnew; Ej = Enew;

end

```

```

function [HPinout] = heatpump(Weather, HPinout)
%Assumption: performance data available, z=f(x^2, y^3)
%           where x = Tshp,o & y = Ta
%Data for: Mitsubishi Ecodan PUHZ-SW200YKA-BS

%Initialisation:
x = HPinout(1); y = Weather(1);
Perf = zeros(3,2); % dummy matrix for [Qth,COP] 1: max, 2:
med, 3: min

%Heat Pump performance data:
%Parameters: coefficients table (9 coefficients for each
surface)
%   MAX CAPACITY: Qmax = const, so coefficients only for
COPmax
C_Qth(1,:) = [6.575 0.6004 1.806 -0.006929 -0.02827 0.02947
0.0002438 ...
-0.00004332 0.00117]; % max capacity of the HP, in kW
C_COP(1,:) = [4.602 -0.04218 0.1834 -0.00006424 -0.003161
0.002288 ...
0.00001778 -0.000006721 -0.0001289]; %COP,max
%   MED CAPACITY:
C_Qth(2,:) = [12.12 0.2894 0.9644 -0.003148 -0.01328 0.02387
...
0.0001894 -0.0002344 -0.0002948]; %Qth,hp,med
C_COP(2,:) = [7.361 -0.1579 -1.159 0.001152 0.04903 0.007806
...
-0.0004878 -0.00007534 0.0001407]; %COP,med
%   MIN CAPACITY:
C_Qth(3,:) = [16.26 -0.03488 0.376 0.005719 0.01868 -
0.00001579...
-0.0002503 -0.0001744 -0.0002503]; %Qth,hp,min
C_COP(3,:) = [5.638 -0.0818 0.3431 0.0002041 -0.008918
0.009047...
0.00006888 -0.00004271 -0.0002597]; %COP,min

%Calculate Qhp,th(t)=f(Tshp,o, Ta): HPinout(3) = ... to check
modulation
%   and COP(t)=f(Tshp,o, Ta): HPinout(4) = ..., for all
capacity levels
for m=1:1:3;
    Perf(m,1) = C_Qth(m,1) + C_Qth(m,2)*x + C_Qth(m,3)*y + ...
        C_Qth(m,4)*x^2 + C_Qth(m,5)*x*y + C_Qth(m,6)*y^2 + ...
        C_Qth(m,7)*x^2*y + C_Qth(m,8)*x*y^2 + C_Qth(m,9)*y^3;

    Perf(m,2) = C_COP(m,1) + C_COP(m,2)*x + C_COP(m,3)*y + ...
        C_COP(m,4)*x^2 + C_COP(m,5)*x*y + C_COP(m,6)*y^2 + ...
        C_COP(m,7)*x^2*y + C_COP(m,8)*x*y^2 + C_COP(m,9)*y^3;
end

if (HPinout(3)>Perf(1,1)); %Qth>Qmax
    HPinout(3) = Perf(1,1); %Qth=Qmax
    HPinout(4) = Perf(1,2); %COP=COPmax
elseif ((Perf(1,1)-HPinout(3))<=0.1); %Qth close to Qmax
    HPinout(4) = Perf(1,2); %COP=COPmax
else % Qmin < Qth <=Qmed

```

```

        if ((HPinout(3)<=Perf(3,1)) || (abs(HPinout(3) -
Perf(3,1))<=0.1)); %Qth close to Qmin
            HPinout(4) = Perf(3,2); %COP=COPmin
        elseif
((HPinout(3)<=Perf(3,1)) || (abs(HPinout(3)-Perf(2,1))<=0.1));
%Qth close to Qmed
            HPinout(4) = Perf(2,2); %COP=COPmed
        else % Qmed < Qth < Qmax
            HPinout(4) = Perf(2,2); %COP=COPmed
        end
    end
end

%calculate mod level:
HPinout(2) = 100*HPinout(3)/Perf(1,1); % mod=100*Qth/Qmax

end

```